understanding sympathetic baroreflex control of arterial pressure. Am J Physiol Heart Circ Physiol 276:H2251–H2261
22. Kawada T, Shishido T, Inagaki M, Zheng C, Yanagiya Y, Uemura K, Sugimachi M, Sunagawa K (2002) Estimation of baroreflex gain using a baroreflex equilibrium diagram. Jpn J Physiol 52:21–29
23. Kashihara K, Takahashi Y, Chatani K, Kawada T, Zheng C, Li M, Sugimachi M, Sunagawa K (2003) Intravenous angiotensin II does not affect dynamic baroreflex characteristics of the neural or peripheral arc. Jpn J Physiol 53:135–143
24. Sanderford MG, Bishop VS (2002) Central mechanisms of acute ANG II modulation of arterial baroreflex control of renal sympathetic nerve activity. Am J Physiol Heart Circ Physiol 282:H1592–H1602
25. Fukiyama K (1972) Central action of angiotensin and hypertension—increased central vasomotor outflow by angiotensin. Jpn Circ J 36:599–602
26. Guo GB, Abboud FM (1984) Angiotensin II attenuates baroreflex control of heart rate and sympathetic activity. Am J Physiol Heart Circ Physiol 246:H80–H89
27. Kamiya A, Kawada T, Yamamoto K, Michikami D, Ariumi H, Uemura K, Zheng C, Shimizu S, Aiba T, Miyamoto T, Sugimachi M, Sunagawa K (2005) Resetting of the arterial baroreflex increases orthostatic sympathetic activation and prevents postural hypotension in rabbits. J Physiol 566:237–246
28. Yamamoto K, Kawada T, Kamiya A, Takaki H, Miyamoto T, Sugimachi M, Sunagawa K (2004) Muscle mechanoreflex induces the pressor response by resetting the arterial baroreflex neural arc. Am J Physiol Heart Circ Physiol 286:H1382–H1388
29. Lumbers ER, McCloskey DI, Potter EK (1979) Inhibition by angiotensin II of baroreceptor-evoked activity in cardiac vagal efferent nerves in the dog. J Physiol 294:69–80
30. Hughes J, Roth RH (1971) Evidence that angiotensin enhances transmitter release during sympathetic nerve stimulation. Br J Phrmacol 41:239–255
31. Zimmerman BG, Gomer SK, Liao JC (1972) Action of angiotensin on vascular adrenergic nerve endings: facilitation of norepinephrine release. Federation Proc 31:1344–1350
32. Reid IA, Chou L (1990) Analysis of the action of angiotensin II on the baroreflex control of heart rate in conscious rabbits. Endocrinology 126:2749–2756
33. Brooks VL (1995) Chronic infusion of angiotensin II resets baroreflex control of heart rate by an arterial pressure-independent mechanism. Hypertension 26:420–424
34. Schunkert H, Tang SS, Litwin SE, Diamant D, Riegger G, Dzau VJ, Ingelfinger JR (1993) Regulation of intrarenal and circulating renin–angiotensin systems in severe heart failure in the rat. Cardiovasc Res 27:731–735
35. Brown AJ, Casals-Stenzel J, Gofford S, Lever AF, Morton JJ (1981) Comparison of fast and slow pressor effects of angiotensin II in the conscious rat. Am J Physiol Heart Circ Physiol 241:H381–H388

Life Sciences 85 (2009) 597–601

Contents lists available at ScienceDirect

Life Sciences

journal homepage: www.elsevier.com/locate/lifescie

Detection of endogenous acetylcholine release during brief ischemia in the rabbit ventricle: A possible trigger for ischemic preconditioning

Toru Kawada [a,*], Tsuyoshi Akiyama [b], Shuji Shimizu [a], Atsunori Kamiya [a], Kazunori Uemura [a], Meihua Li [a], Mikiyasu Shirai [b], Masaru Sugimachi [a]

[a] Department of Cardiovascular Dynamics, Advanced Medical Engineering Center, National Cardiovascular Center Research Institute, Japan
[b] Department of Cardiac Physiology, National Cardiovascular Center Research Institute, Japan

ARTICLE INFO

Article history:
Received 1 July 2009
Accepted 25 August 2009

Keywords:
Acetylcholine
Cardiac microdialysis
Vagal stimulation
Coronary artery occlusion
Rabbits

ABSTRACT

Aims: To examine endogenous acetylcholine (ACh) release in the rabbit left ventricle during acute ischemia, ischemic preconditioning and electrical vagal stimulation.
Main methods: We measured myocardial interstitial ACh levels in the rabbit left ventricle using a cardiac microdialysis technique. In Protocol 1 ($n=6$), the left circumflex coronary artery (LCX) was occluded for 30 min and reperfused for 30 min. In Protocol 2 ($n=5$), the LCX was temporarily occluded for 5 min. Ten minutes later, the LCX was occluded for 30 min and reperfused for 30 min. In Protocol 3 ($n=5$), bilateral efferent vagal nerves were stimulated at 20 Hz and 40 Hz (10 V, 1-ms pulse duration).
Key findings: In Protocol 1, a 30-min coronary occlusion increased the ACh level from 0.39 ± 0.15 to 7.0 ± 2.2 nM (mean ± SE, $P<0.01$). In Protocol 2, a 5-min coronary occlusion increased the ACh level from 0.33 ± 0.07 to 0.75 ± 0.11 nM ($P<0.05$). The ACh level returned to 0.48 ± 0.10 nM during the interval. After that, a 30-min coronary occlusion increased the ACh level to 2.4 ± 0.49 nM ($P<0.01$). In Protocol 3, vagal stimulation at 20 Hz and 40 Hz increased the ACh level from 0.29 ± 0.06 to 1.23 ± 0.48 ($P<0.05$) and 2.44 ± 1.13 nM ($P<0.01$), respectively.
Significance: Acute ischemia significantly increased the ACh levels in the rabbit left ventricle, which appeared to exceed the vagal stimulation-induced ACh release. Brief ischemia as short as 5 min can also increase the ACh level, suggesting that endogenous ACh release can be a trigger for ischemic preconditioning.

Introduction

Although ventricular vagal innervation is sparser than that observed in the atrium, we have previously demonstrated that electrical vagal stimulation and acute myocardial ischemia significantly increased myocardial interstitial acetylcholine (ACh) levels in the feline left ventricle (Kawada et al. 2000, 2001, 2006a,b, 2007). Potential differences between species, however, suggest that data obtained from the feline left ventricle may not be directly extrapolated to ventricular vagal innervation in other species (Brown 1976; Kilbinger and Löffelholz 1976). Compared with the feline heart, the rabbit heart is more frequently analyzed in investigations of myocardial ischemia and ischemic preconditioning. For instance, Qin et al. (2003) used isolated rabbit hearts to demonstrate that ACh and adenosine induce ischemic preconditioning mimetic effects through different signaling pathways. In our previous study, vagal stimulation increased the level of tissue inhibitor of metalloproteinase-1 (TIMP-1) and reduced the level of endogenous active matrix metalloproteinase-9 (MMP-9) during ischemia–reperfusion injury in the rabbit left ventricle (Uemura et al. 2007). Despite its potential cardioprotective effects against myocardial ischemia, the profile of endogenous ACh release in the rabbit left ventricle is poorly understood *in vivo* owing to the difficulty in detecting low levels of myocardial interstitial ACh. Quantification of endogenous ACh release during myocardial ischemia and electrical vagal stimulation would help understand the potential cardioprotective effects of vagal stimulation. In the present study, we examined the effects of acute myocardial ischemia, ischemic preconditioning, and electrical vagal stimulation on myocardial interstitial ACh levels in the rabbit left ventricle *in vivo* using an improved high-performance liquid chromatography (HPLC) system that allowed us to detect low concentrations of ACh (Shimizu et al. 2009).

Materials and methods

Surgical preparation and protocols

Animal care was conducted in accordance with the *Guiding Principles for the Care and Use of Animals in the Field of Physiological Sciences*, which has been approved by the Physiological Society of

* Corresponding author. Department of Cardiovascular Dynamics, Advanced Medical Engineering Center, National Cardiovascular Center Research Institute, 5-7-1 Fujishirodai, Suita, Osaka 565-8565, Japan. Tel.: +81 6 6833 5012x2427; fax: +81 6 6835 5403.
E-mail address: torukawa@res.ncvc.go.jp (T. Kawada).

0024-3205/$ – see front matter © 2009 Published by Elsevier Inc.
doi:10.1016/j.lfs.2009.08.015

Japan. Japanese white rabbits weighing 2.5 kg to 3.1 kg (2.8 ± 0.1 kg, mean ± SE) were anesthetized via intravenous administration of pentobarbital sodium (30–35 mg/kg) through a marginal ear vein. The animals were ventilated mechanically with room air mixed with oxygen. The anesthetic condition was maintained using a continuous intravenous infusion of urethane (125 mg kg^{-1} h^{-1}) and α-chloralose (20 mg kg^{-1} h^{-1}) through a catheter inserted in the right femoral vein. Mean arterial pressure (AP) was measured using a catheter inserted in the right femoral artery. Heart rate (HR) was measured from an electrocardiogram obtained using a cardiotachometer. The animal was placed in a lateral position, and the left fourth and fifth ribs were partially resected to allow access to the heart. The heart was suspended in a pericardial cradle.

In Protocol 1 ($n=6$), which was designed to examine the effects of acute myocardial ischemia and reperfusion, a 3-0 silk suture was passed around a branch of the left circumflex coronary artery (LCX); both ends were passed through a polyethylene tube to make a snare to occlude the artery. A dialysis probe was implanted into the anterolateral free wall of the left ventricle perfused by the LCX. After collecting a baseline dialysate sample, the LCX was occluded for 30 min and reperfused for 30 min. After the ischemia–reperfusion protocol was finished, the LCX was occluded again and a 5-ml bolus of 1% methylene blue was injected intravenously to confirm that the dialysis probe had been implanted within the area at risk for myocardial ischemia.

In Protocol 2 ($n=5$), which was designed to examine the effects of ischemic preconditioning (*i.e.*, a brief ischemic event preceding a major ischemic event), a 3-0 silk suture was passed around a branch of the LCX and both ends were passed through a polyethylene tube to make a snare. Two dialysis probes were implanted into the anterolateral free wall of the left ventricle perfused by the LCX; the probes were separated by at least 5 mm. Combining the dialysate samples obtained from the two dialysis probes increased the time resolution of the ACh measurement. After collecting a baseline dialysate sample, the LCX was temporarily occluded for 5 min which was followed by a 10-min interval. The LCX was then occluded for 30 min and reperfused for 30 min. After the ischemia–reperfusion protocol was completed, the LCX was occluded again and a 5-ml bolus of 1% methylene blue was injected intravenously to confirm that the two dialysis probes had been implanted within the area at risk for myocardial ischemia.

In Protocol 3 ($n=5$), which was designed to examine the effects of electrical vagal stimulation, the vagus nerves were exposed and sectioned at the neck. Each sectioned vagus nerve was placed on a pair of bipolar platinum electrodes to stimulate the efferent vagus nerve. The nerve and the electrodes were fixed using silicone glue (Kwik-Sil, World Precision Instruments, Sarasota, FL, USA). Two dialysis probes were implanted into the anterolateral free wall of the left ventricle; the probes were separated by at least 5 mm. Dialysate samples obtained from the two dialysis probes were analyzed separately. After collecting baseline dialysate samples, the vagus nerves were stimulated at 20 Hz for 15 min and 40 Hz for 15 min. The stimulation amplitude was 10 V and the pulse duration was 1 ms. The 40-Hz stimulation often caused an initial cardiac arrest for a few seconds and was considered to be the most intensive stimulation in the present experimental settings. The 20-Hz stimulation was arbitrarily selected at a half of the maximum stimulation rate to observe the dependence of the ACh release on the stimulation rate.

At the end of each protocol, the experimental animals were sacrificed with an overdose of intravenous pentobarbital sodium. We performed a postmortem examination and confirmed that the dialysis probe(s) had been implanted within the left ventricular myocardium.

Dialysis technique

We measured dialysate concentrations of ACh as indices of myocardial interstitial ACh levels. The materials and properties of the dialysis probe have been described previously (Akiyama et al. 1994). Briefly, we designed a transverse dialysis probe. A dialysis fiber (length, 8 mm; outer diameter, 310 μm; inner diameter, 200 μm; PAN-1200, 50,000-Da molecular-weight cutoff, Asahi Chemical, Japan) was glued at both ends to polyethylene tubes (length, 25 cm; outer diameter, 500 μm; inner diameter, 200 μm). The dialysis probe was perfused at a rate of 2 μl/min with Ringer's solution containing a cholinesterase inhibitor eserine (100 μM). Dialysate sampling was started from 2 h after probe implantation. In Protocols 1 and 3, one sampling period was set at 15 min, which yielded a sample volume of 30 μl. The actual dialysate sampling lagged behind a given collection period by 5 min owing to the dead space volume between the dialysis membrane and collecting tube. In Protocol 2, one sampling period was set at 5 min to increase the time resolution during the ischemic preconditioning, and dialysate samples from the two dialysis probes were combined to yield a sample volume of 20 μl. The sampling period was changed to 10 min during the main ischemic event to reduce the total number of samples. The amount of ACh in the dialysate was measured using an HPLC system with electrochemical detection (Eicom, Japan) adjusted to measure low levels of ACh (Shimizu et al. 2009). The concentration of ACh was calculated taking the sample volume in account.

Statistical analysis

All data are presented as the mean and SE values. We performed repeated-measures analysis of variance, followed by a Tukey test for all pairwise, multiple comparisons to examine changes in the ACh levels (Glantz 2002). Because the variance of measured ACh levels increased with their mean, statistical analysis was performed after logarithmic conversion of the ACh data (Snedecor and Cochran 1989). The AP and HR data were examined using repeated-measures analysis of variance, followed by a Dunnett's test for multiple comparisons against a single control (Glantz 2002). In Protocols 1 and 3, the baseline value was treated as the single control. In Protocol 2, the value measured just before the main ischemic event was treated as the single control. In all of the statistical analyses, differences were considered significant when $P<0.05$.

Results

In Protocol 1, the myocardial interstitial ACh levels significantly increased during ischemia compared with the baseline value (Fig. 1). Although the ACh levels declined during reperfusion, they were still significantly higher than the baseline value. Changes in AP and HR are summarized in Table 1. Although AP did not change significantly during ischemia, it decreased significantly throughout the reperfusion period. The HR increased significantly after 30 min of ischemia, and remained high during the reperfusion period with the exception of the last data point.

In Protocol 2, the LCX was occluded for 5 min (ischemic preconditioning) and released for 10 min before the major ischemic event. The brief 5-min occlusion significantly increased the myocardial interstitial ACh level compared with the baseline value (Fig. 2). The ACh levels during the interval between the brief occlusion and the major occlusion did not differ from the baseline value. The ACh levels increased significantly during the major ischemic event compared with the baseline value. Although the ACh levels declined during reperfusion, they were still significantly higher than the baseline value. Changes in AP and HR are summarized in Table 2. Neither AP nor HR changed significantly compared with the respective control values measured after the 10-min middle interval.

In Protocol 3, electrical vagal stimulation significantly increased the myocardial interstitial ACh levels (Fig. 3). The ACh levels returned close to the baseline value just after vagal stimulation was terminated. The AP and HR values were significantly reduced by vagal stimulation (Table 3).

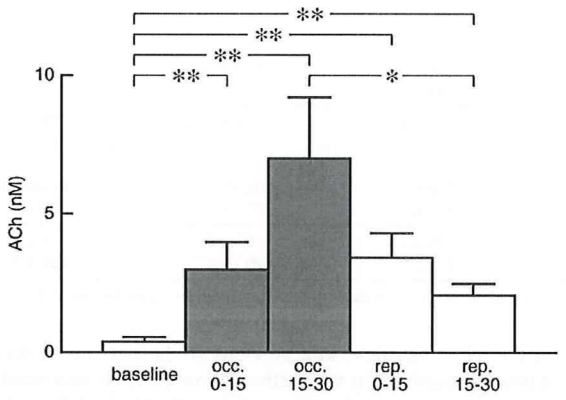

Fig. 1. Changes in the myocardial interstitial ACh levels in Protocol 1. The left circumflex coronary artery was occluded for 30 min and reperfused for 30 min. occ: occlusion; rep: reperfusion. Data are shown as the mean + SE ($n=6$). *$P<0.05$ and **$P<0.01$; Tukey test.

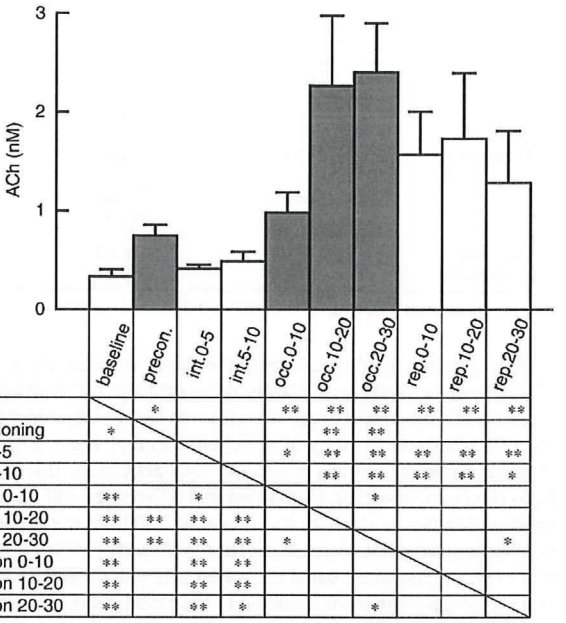

Fig. 2. Changes in the myocardial interstitial ACh levels in Protocol 2. The left circumflex coronary artery was occluded for 5 min. Ten minutes later, the left circumflex coronary artery was occluded for 30 min and reperfused for 30 min. precon: preconditioning; int: interval; occ: occlusion; rep: reperfusion. Data are shown as the mean + SE ($n=5$). *$P<0.05$ and **$P<0.01$; Tukey test.

Discussion

Effects of acute ischemia on myocardial interstitial ACh levels

Acute myocardial ischemia significantly increased myocardial interstitial ACh levels in the ischemic region (Fig. 1). To our knowledge, this is the first report demonstrating ischemia-induced ACh release in the rabbit left ventricle *in vivo*. Because electrical vagal stimulation increased the myocardial interstitial ACh levels (Fig. 3), centrally mediated activation of the efferent vagus nerve could contribute to these effects. LCX occlusion, however, did not decrease the HR significantly (Table 1), suggesting that centrally mediated vagal activation did not have a marked role in the present study. In a previous study, acute myocardial ischemia increased myocardial interstitial ACh levels in vagotomized cats, suggesting an important role of a local release mechanism that is independent of efferent vagal activity (Kawada et al. 2000). Intracellular Ca^{2+} mobilization related to cation-selective stretch-activated channels is thought to be involved in this local release mechanism (Kawada et al. 2000, 2006b). A similar local mechanism may be responsible for ischemia-induced ACh release in the rabbit left ventricle.

In our previous study, topical perfusion of ACh through a dialysis probe increased TIMP-1 levels in the rabbit left ventricle (Uemura et al. 2007). The production of TIMP-1 reduces endogenous levels of active MMP-9, which can limit ventricular remodeling following myocardial ischemia and reperfusion. Whether ischemia-induced ACh release can induce such an anti-remodeling effect remains unanswered, however, because reperfusion reduced the myocardial interstitial ACh levels toward the baseline value. Whether prolonged ischemia for more than 30 min induces sustained elevations of ACh levels is an interesting topic for future studies.

The ACh levels were decreased toward the baseline value upon reperfusion, probably by the washout of ACh from the interstitial fluid. In the case of myocardial interstitial myoglobin levels, the reperfusion further increases the myoglobin levels, suggesting an occurrence of reperfusion injury to the myocardium (Kitagawa et al. 2005). Reoxygenation upon reperfusion rapidly restores the ATP synthesis, which can cause hypercontracture of myofibrils and undesired cytoskeletal lesions (Piper et al. 2004). Because the vagal nerve endings do not have contractile elements, the hypercontracture-induced cell injury does not occur, and the further release of ACh may have been prevented.

Effects of ischemic preconditioning on myocardial interstitial ACh levels

Ischemic preconditioning is a phenomenon in which a brief ischemic event makes the heart resistant to a subsequent ischemic insult (Murry et al. 1986). Acetylcholine, bradykinin, and adenosine are endogenous substances that can induce ischemic preconditioning mimetic effects in the rabbit heart (Liu et al. 1991; Qin et al. 2003; Krieg et al. 2004). In a previous study, we showed that a 5-min ischemic event increased myocardial interstitial ACh levels in the feline ventricle (Kawada et al. 2002). Ischemic preconditioning, however, is not frequently examined in the feline ventricle, making interpretation of these results difficult. In the present study, a 5-min ischemic event caused a significant increase in the ACh level in the rabbit left ventricle (Fig. 2), suggesting that brief ischemia-induced ACh release may serve as a trigger for the ischemic preconditioning. Krieg et al. (2004) demonstrated that ACh triggers preconditioning by sequentially activating Akt and nitric oxide synthase to produce reactive oxygen species. An acetylcholine-induced preconditioning mimetic effect has also been observed in canine (Yao and Gross 1993; Przyklenk and Kloner 1995) and rat (Richard et al. 1995) models.

Table 1
Mean arterial pressure (AP) and heart rate (HR) obtained during Protocol 1 ($n=6$).

	Baseline	Occlusion 5 min	Occlusion 15 min	Occlusion 30 min	Reperfusion 5 min	Reperfusion 15 min	Reperfusion 30 min
AP(mm Hg)	82±4	77±4	72±5	75±5	72±5*	70±4*	70±2**
HR (beats/min)	247±16	264±14	265±13	280±10**	278±9*	277±8*	274±9

Data are shown as the mean±SE. *$P<0.05$ and **$P<0.01$ vs. baseline using Dunnett's test.

Table 2
Mean arterial pressure (AP) and heart rate (HR) obtained during Protocol 2 ($n=5$).

	Baseline	Preconditioning 5 min	Interval 5 min	Interval 10 min	Occlusion 5 min	Occlusion 10 min
AP(mm Hg)	83±5	77±5	78±4	80±4	78±5	78±5
HR(beats/min)	277±7	282±8	282±7	284±5	285±5	286±6
	Occlusion 20 min	Occlusion 30 min	Reperfusion 5 min	Reperfusion 10 min	Reperfusion 20 min	Reperfusion 30 min
AP(mm Hg)	77±4	78±5	77±5	78±5	77±3	79±3
HR(beats/min)	287±5	289±6	290±5	289±5	290±6	293±5

Data are shown as the mean±SE. No significant differences relative to control values (the value 10 min after the preconditioning) were observed based on Dunnett's test.

In a previous study examining the feline ventricle (Kawada et al. 2002), brief ischemia significantly decreased the HR, highlighting the presence of a significant vagal reflex from the heart. Vagotomy abolished the ACh release induced by brief ischemia in that study, suggesting an important role of centrally mediated vagal activation. The vagal reflex from the heart, however, shows regional differences and varies among species (Thames et al. 1978; Kawada et al. 2007). In the present study, brief ischemia did not decrease the HR significantly (Table 2), suggesting that centrally mediated vagal activation was not a major factor for the brief ischemia-induced ACh release in the rabbit heart.

Rabbits exhibit marked effects from ischemic preconditioning, including reduced infarct size (Cohen et al. 1991; Cason et al. 1997). Although whether the ACh release induced by the brief ischemic event exerted cardioprotective effects was not examined in the present study, there was a notable difference in the changes in AP observed with Protocol 1 and Protocol 2. Although AP decreased significantly upon reperfusion in Protocol 1 (Table 1), it did not change significantly during the major ischemic event in Protocol 2 (Table 2), possibly reflecting preserved cardiac function as a result of the ischemic preconditioning.

Effects of electrical vagal stimulation on myocardial interstitial ACh levels

In the feline left ventricle, electrical vagal stimulation at 20 Hz (10 V, 1-ms pulse duration) increases myocardial interstitial ACh levels to approximately 20 nM as measured with a dialysis fiber 13 mm in length (Kawada et al. 2000). In contrast, electrical vagal stimulation at 20 Hz in the rabbit left ventricle (10 V, 1-ms pulse duration) increased the ACh levels to approximately 1.2 nM as measured with a dialysis fiber 8 mm long (Fig. 3). The small increase in the ACh level detected during electrical vagal stimulation may indicate that vagal innervation is much sparser in the rabbit ventricle

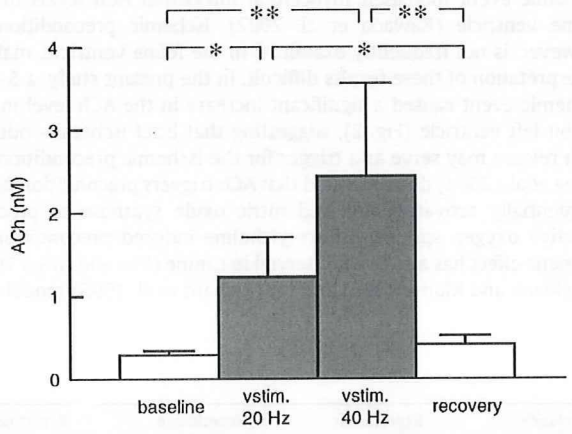

Fig. 3. Changes in the myocardial interstitial ACh levels in Protocol 3. The bilateral efferent vagus nerves were stimulated at 20 Hz for 15 min and 40 Hz for 15 min. Data are shown as the mean+SE ($n=10$, 2 samples from each of the 5 animals). *$P<0.05$ and **$P<0.01$; Tukey test.

than in the feline ventricle. In a previous study that used a dialysis fiber 4 mm in length, right vagal stimulation at 20 Hz increased the dialysate ACh concentration from 0.4±0.2 nM to 0.9±0.3 nM, whereas left vagal stimulation at 20 Hz increased it from 0.3±0.1 nM to 1.0±0.4 nM in the rabbit right ventricle (Shimizu et al. 2009). Considering the bilateral stimulation and fiber length of 8 mm in the present study, the vagal innervation of the left ventricle may be comparable to or slightly sparser than that of the right ventricle.

The dialysis fiber differed in length among studies due to anatomical restrictions related to the fiber implantation procedure (*i.e.*, size of the heart etc.). If we consider diffusive processes alone, the relative recovery (RR) can be expressed as:

$$RR = \frac{C_{inside}}{C_{outside}} = 1 - \exp\left(-k\frac{A}{F}\right) = 1 - \exp\left(-k\frac{mL}{F}\right)$$

where C_{inside} and $C_{outside}$ are the ACh concentrations inside and outside the dialysis fiber; A is the surface area of the dialysis membrane, which can be proportional to the fiber length L with a coefficient m; F is a perfusion flow rate; and k is the mass transfer coefficient (Ståhle 1991). The *in vitro* RR for ACh is approximately 70% with $F=2$ µl/min and $L=13$ mm (Akiyama et al. 1994), which yields $km=0.1852$. Using this value, the *in vitro* RR would be approximately 52% for $L=8$ mm and 31% for $L=4$ mm. Although these values provide some clues to speculate the effects of fiber length on the detected ACh concentrations, they cannot be directly extrapolated to the present results, because k should be different in *in vivo* conditions.

The physiological significance of vagal innervation of the left ventricle is controversial, because fixed-rate atrial pacing abolishes vagally induced inhibition of left ventricular contractility in an experimental setting without significant background sympathetic tone (Matsuura et al. 1997). On the other hand, when the cardiac sympathetic nerve is activated, vagal stimulation can reduce ventricular contractility even under fixed-rate atrial pacing by antagonizing the sympathetic effect (Nakayama et al. 2001). In addition, vagal stimulation suppresses myocardial interstitial myoglobin release during acute myocardial ischemia in anesthetized cats (Kawada et al. 2008). Chronic vagal stimulation improves the survival rate of rat models of chronic heart failure after myocardial infarction (Li et al. 2004). These lines of evidence suggest that vagal innervation of the left ventricle may be of therapeutic significance.

An unresolved question regarding the cardioprotective effects of vagal stimulation is that a large quantity of ACh is released in the ischemic region without vagal stimulation (Fig. 1). In the present

Table 3
Mean arterial pressure (AP) and heart rate (HR) obtained during Protocol 3 ($n=5$).

	Baseline	Vagal stimulation 20 Hz	Vagal stimulation 40 Hz	Recovery
AP (mm Hg)	100±3	59±9**	54±9**	86±5
HR (beats/min)	322±14	126±5**	100±8**	311±8

Data are shown as the mean±SE. **$P<0.01$ vs. baseline based on Dunnett's test.

study, vagal stimulation at 20-Hz lowered the HR by approximately 200 beats/min (to less than 40% of the control value) but the stimulation-induced ACh release did not exceed the ischemia-induced ACh release (Figs. 1 and 3). On the other hand, vagal stimulation that reduced the HR by only 10% produces a significant increase in the survival rate of chronic heart failure rats (Li et al. 2004). Therefore, vagal stimulation probably exerts its beneficial effects not only within the ischemic region but also outside of this region. For instance, vagal stimulation in dogs with a healed myocardial infarction is known to prevent lethal arrhythmia induced by exercise (Vanoli et al. 1991). Afferent vagal activation may also contribute to the cardioprotective effects. Further studies are clearly needed to identify the mechanisms underlying the vagally induced cardioprotective effects against myocardial infarction and chronic heart failure.

Conclusion

The present study demonstrated the presence of vagal innervation in the rabbit left ventricle. Acute myocardial ischemia significantly increased the myocardial interstitial ACh levels. In addition, a brief ischemic event (5 min) caused detectable increases in ACh levels, indicating that endogenous ACh release may provide a trigger for ischemic preconditioning.

Acknowledgments

This study was supported by the Health and Labour Sciences Research Grants (H18-nano-Ippan-003, H19-nano-Ippan-009, H20-katsudo-Shitei-007, and H21-nano-Ippan-005) from the Ministry of Health, Labour and Welfare of Japan; by a Grant-in-Aid for Scientific Research (No. 20390462) from the Ministry of Education, Culture, Sports, Science and Technology of Japan; and by the Industrial Technology Research Grant Program from the New Energy and Industrial Technology Development Organization (NEDO) of Japan.

References

Akiyama T, Yamazaki T, Ninomiya I. In vivo detection of endogenous acetylcholine release in cat ventricles. American Journal of Physiology 266 (3 Pt 2), H854–H860, 1994.

Brown OM. Cat heart acetylcholine: Structural proof and distribution. American Journal of Physiology 231 (3), 781–785, 1976.

Cason BA, Gamperl AK, Slocum RE, Hickey RF. Anesthetic-induced preconditioning: Previous administration of isoflurane decreases myocardial infarct size in rabbits. Anesthesiology 87 (5), 1182–1190, 1997.

Cohen MV, Liu GS, Downey JM. Preconditioning causes improved wall motion as well as smaller infarcts after transient coronary occlusion in rabbits. Circulation 84 (1), 341–349, 1991.

Glantz SA. Primer of Biostatistics, 5th ed. McGraw-Hill, New York, 2002.

Kawada T, Yamazaki T, Akiyama T, Sato T, Shishido T, Inagaki M, Takaki H, Sugimachi M, Sunagawa K. Differential acetylcholine release mechanisms in the ischemic and non-ischemic myocardium. Journal of Molecular and Cellular Cardiology 32 (3), 405–414, 2000.

Kawada T, Yamazaki T, Akiyama T, Shishido T, Inagaki M, Uemura K, Miyamoto T, Sugimachi M, Takaki H, Sunagawa K. In vivo assessment of acetylcholine releasing function at cardiac vagal nerve terminals. American Journal of Physiology. Heart and Circulatory Physiology 281 (1), H139–H145, 2001.

Kawada T, Yamazaki T, Akiyama T, Mori H, Inagaki M, Shishido T, Takaki H, Sugimachi M, Sunagawa K. Effects of brief ischaemia on myocardial acetylcholine and noradrenaline levels in anaesthetized cats. Autonomic Neuroscience: Basic and Clinical 95 (1–2), 37–42, 2002.

Kawada T, Yamazaki T, Akiyama T, Li M, Ariumi H, Mori H, Sunagawa K, Sugimachi M. Vagal stimulation suppresses ischemia-induced myocardial interstitial norepinephrine release. Life Sciences 78 (8), 882–887, 2006a.

Kawada T, Yamazaki T, Akiyama T, Uemura K, Kamiya A, Shishido T, Mori H, Sugimachi M. Effects of Ca^{2+} channel antagonists on nerve stimulation-induced and ischemia-induced myocardial interstitial acetylcholine release in cats. American Journal of Physiology. Heart and Circulatory Physiology 291 (5), H2187–H2191, 2006b.

Kawada T, Yamazaki T, Akiyama T, Shishido T, Shimizu S, Mizuno M, Mori H, Sugimachi M. Regional difference in ischaemia-induced myocardial interstitial noradrenaline and acetylcholine releases. Autonomic Neuroscience: Basic and Clinical 137 (1–2), 44–50, 2007.

Kawada T, Yamazaki T, Akiyama T, Kitagawa H, Shimizu S, Mizuno M, Li M, Sugimachi M. Vagal stimulation suppresses ischemia-induced myocardial interstitial myoglobin release. Life Sciences 83 (13–14), 490–495, 2008.

Kilbinger H, Löffelholz K. The isolated perfused chicken heart as a tool for studying acetylcholine output in the absence of cholinesterase inhibition. Journal of Neural Transmission 38, 9–14, 1976.

Kitagawa H, Yamazaki T, Akiyama T, Sugimachi M, Sunagawa K, Mori H. Microdialysis separately monitors myocardial interstitial myoglobin during ischemia and reperfusion. American Journal of Physiology Heart and Circulatory Physiology 289 (2), H924–H930, 2005.

Krieg T, Qin Q, Philipp S, Alexeyev MF, Cohen MV, Downey JM. Acetylcholine and bradykinin trigger preconditioning in the heart through a pathway that induces Akt and NOS. American Journal of Physiology. Heart and Circulatory Physiology 287 (6), H2606–H2611, 2004.

Li M, Zheng C, Sato T, Kawada T, Sugimachi M, Sunagawa K. Vagal nerve stimulation markedly improves long-term survival after chronic heart failure in rats. Circulation 109 (1), 120–124, 2004.

Liu GS, Thornton J, Van Winkle DM, Stanley AW, Olsson RA, Downey JM. Protection against infarction afforded by preconditioning is mediated by A_1 adenosine receptors in rabbit heart. Circulation 84 (1), 350–356, 1991.

Matsuura W, Sugimachi M, Kawada T, Sato T, Shishido T, Miyano H, Nakahara T, Ikeda Y, Alexander Jr J, Sunagawa K. Vagal stimulation decreases left ventricular contractility mainly through negative chronotropic effect. American Journal of Physiology 273 (2 Pt 2), H534–H539, 1997.

Murry CE, Jennings RB, Reimer KA. Preconditioning with ischemia: A delay of lethal cell injury in ischemic myocardium. Circulation 74 (5), 1124–1136, 1986.

Nakayama Y, Miyano H, Shishido T, Inagaki M, Kawada T, Sugimachi M, Sunagawa K. Heart rate-independent vagal effect on end-systolic elastance of the canine left ventricle under various levels of sympathetic tone. Circulation 104 (19), 2277–2279, 2001.

Piper HM, Abdallah Y, Schäfer C. The first minutes of reperfusion: A window of opportunity for cardioprotection. Cardiovascular Research 61 (3), 365–371, 2004.

Przyklenk K, Kloner RA. Low-dose iv acetylcholine acts as a "preconditioning-mimetic" in the canine model. Journal of Cardiac Surgery 10 (4), 389–395, 1995.

Qin Q, Downey JM, Cohen MV. Acetylcholine but not adenosine triggers preconditioning through PI3-kinase and a tyrosine kinase. American Journal of Physiology. Heart and Circulatory Physiology 284 (2), H727–H734, 2003.

Richard V, Blanc T, Kaeffer N, Tron C, Thuillez C. Myocardial and coronary endothelial protective effects of acetylcholine after myocardial ischaemia and reperfusion in rats: Role of nitric oxide. British Journal of Pharmacology 115 (8), 1532–1538, 1995.

Shimizu S, Akiyama T, Kawada T, Shishido T, Yamazaki T, Kamiya A, Mizuno M, Sano S, Sugimachi M. In vivo direct monitoring of vagal acetylcholine release to the sinoatrial node. Autonomic Neuroscience: Basic and Clinical 148 (1–2), 44–49, 2009.

Snedecor GW, Cochran WG. Statistical Methods. Iowa State, Iowa, pp. 290–291, 1989.

Ståhle L. The use of microdialysis in pharmacokinetics and pharmacodynamics. In: Robinson, TE, JusticeJr. Jr, JB (Eds.), Microdialysis in the Neurosciences, pp. 155–174. Elsevier Science Ltd. New York, 1991.

Thames MD, Klopfenstein HS, Abboud FM, Mark AL, Walker JL. Preferential distribution of inhibitory cardiac receptors with vagal afferents to the inferoposterior wall of the left ventricle activated during coronary occlusion in the dog. Circulation Research 43 (4), 512–519, 1978.

Uemura K, Li M, Tsutsumi T, Yamazaki T, Kawada T, Kamiya A, Inagaki M, Sunagawa K, Sugimachi M. Efferent vagal nerve stimulation induces tissue inhibitor of metalloproteinase-1 in myocardial ischemia–reperfusion injury in rabbit. American Journal of Physiology. Heart and Circulatory Physiology 293 (4), H2254–H2261, 2007.

Vanoli E, de Ferrari GM, Stramba-Badiale M, Hull Jr SS, Foreman RD, Schwartz PJ. Vagal stimulation and prevention of sudden death in conscious dogs with a healed myocardial infarction. Circulation Research 68 (5), 1471–1481, 1991.

Yao Z, Gross GJ. Acetylcholine mimics ischemic preconditioning via a glibenclamide-sensitive mechanism in dogs. American Journal of Physiology 264 (6 Pt 2), H2221–H2225, 1993.

Metformin Prevents Progression of Heart Failure in Dogs
Role of AMP-Activated Protein Kinase

Hideyuki Sasaki, MD; Hiroshi Asanuma, MD, PhD; Masashi Fujita, MD, PhD; Hiroyuki Takahama, MD, PhD; Masakatsu Wakeno, MD, PhD; Shin Ito, MD; Akiko Ogai, BS; Masanori Asakura, MD, PhD; Jiyoong Kim, MD; Tetsuo Minamino, MD, PhD; Seiji Takashima, MD, PhD; Shoji Sanada, MD, PhD; Masaru Sugimachi, MD, PhD; Kazuo Komamura, MD, PhD; Naoki Mochizuki, MD, PhD; Masafumi Kitakaze, MD, PhD

Background—Some studies have shown that metformin activates AMP-activated protein kinase (AMPK) and has a potent cardioprotective effect against ischemia/reperfusion injury. Because AMPK also is activated in animal models of heart failure, we investigated whether metformin decreases cardiomyocyte apoptosis and attenuates the progression of heart failure in dogs.

Methods and Results—Treatment with metformin (10 μmol/L) protected cultured cardiomyocytes from cell death during exposure to H_2O_2 (50 μmol/L) via AMPK activation, as shown by the MTT assay, terminal deoxynucleotidyl transferase–mediated dUTP nick-end labeling staining, and flow cytometry. Continuous rapid ventricular pacing (230 bpm for 4 weeks) caused typical heart failure in dogs. Both left ventricular fractional shortening and left ventricular end-diastolic pressure were significantly improved in dogs treated with oral metformin at 100 $mg \cdot kg^{-1} \cdot d^{-1}$ (n=8) (18.6±1.8% and 11.8±1.1 mm Hg, respectively) compared with dogs receiving vehicle (n=8) (9.6±0.7% and 22±0.9 mm Hg, respectively). Metformin also promoted phosphorylation of both AMPK and endothelial nitric oxide synthase, increased plasma nitric oxide levels, and improved insulin resistance. As a result of these effects, metformin decreased apoptosis and improved cardiac function in failing canine hearts. Interestingly, another AMPK activator (AICAR) had effects equivalent to those of metformin, suggesting the primary role of AMPK activation in reducing apoptosis and preventing heart failure.

Conclusions—Metformin attenuated oxidative stress–induced cardiomyocyte apoptosis and prevented the progression of heart failure in dogs, along with activation of AMPK. Therefore, metformin may be a potential new therapy for heart failure. (***Circulation.*** **2009;119:2568-2577.)**

Key Words: AMP-activated protein kinase ■ heart failure ■ metformin ■ nitric oxide

Metformin is widely used as an antidiabetic drug with an insulin-sensitizing effect. A large-scale clinical trial (the UK Prospective Diabetes Study [UKPDS] 34) has shown that metformin therapy decreased the risk of cardiovascular death and the incidence of myocardial infarction associated with diabetes mellitus,[1] suggesting that this drug may be useful for patients who have both cardiovascular disease and diabetes mellitus. Eurich and colleagues[2] recently reported the results of a meta-analysis showing that metformin was the only antidiabetic agent to reduce all-cause mortality without causing any harm in patients who had heart failure and diabetes mellitus. These results suggest that a tight link exists between cardiovascular disease and diabetes mellitus and that metformin has a cardioprotective effect. Metformin is known to activate AMP-activated protein kinase (AMPK),[3–5] which is expressed in various tissues, including the myocardium, and plays a central role in the regulation of energy metabolism under stress conditions.[6] AMPK is activated by ischemia/reperfusion,[7–9] as well as in hearts with pressure overload hypertrophy[10] and subsequent heart failure.[11,12] In addition, Russell et al[9] have demonstrated that isolated hearts of AMPK-deleted mice show increased apoptosis and dysfunction after ischemia/reperfusion. Activation of AMPK by adiponectin also has been reported to protect cardiomyocytes against apoptosis and to attenuate myocardial ischemia/reperfusion injury in mice.[8] Furthermore, metformin has been reported to increase the production of nitric oxide (NO),[13–15] which is known to have various beneficial cardiovascular

Received August 23, 2007; accepted February 24, 2009.

From the Department of Cardiovascular Medicine, National Cardiovascular Center (H.S., H.A., H.T., M.W., S.I., A.O., M.A., J.K., K.K., M.K.) and Departments of Structural Analysis (H.S., H.T., M.W., S.I., N.M.) and Cardiovascular Dynamics (M.S., K.K.), Research Institute, National Cardiovascular Center, Suita, Osaka; Departments of Bioregulatory Medicine (H.S., H.T., M.W., S.I., N.M.) and Cardiovascular Medicine (M.F., T.M., S.T., S.S.), Osaka University Graduate School of Medicine, Suita, Osaka, Japan; and Department of Emergency Room Medicine, Kinki University School of Medicine, Osaka-Sayama (H.A.), Osaka, Japan.

The online-only Data Supplement is available with this article at http://circ.ahajournals.org/cgi/content/full/CIRCULATIONAHA.108.798561/DC1.

Correspondence to Masafumi Kitakaze, MD, PhD, Department of Cardiovascular Medicine, National Cardiovascular Center, 5–7–1 Fujishirodai, Suita, Osaka 565–8565, Japan. E-mail kitakaze@zf6.so-net.ne.jp

Circulation **is available at http://circ.ahajournals.org** **DOI: 10.1161/CIRCULATIONAHA.108.798561**

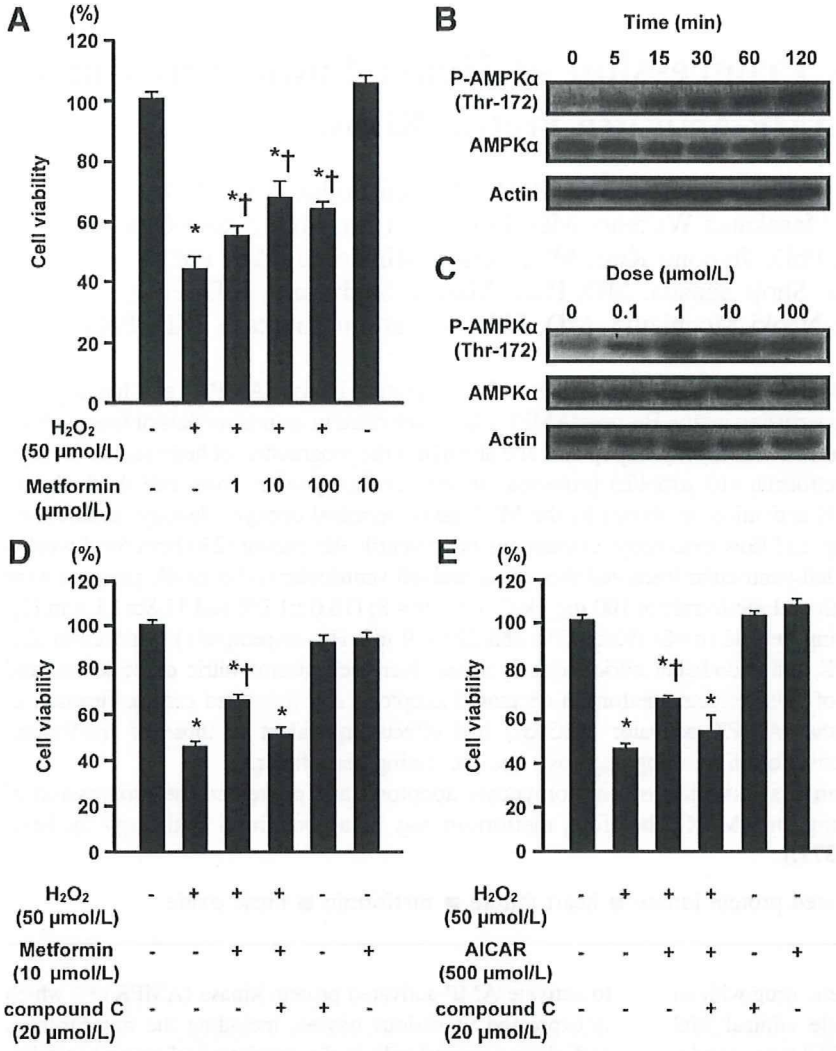

Figure 1. Effect of metformin on oxidative stress–induced cell death via AMPK activation in cultured rat cardiomyocytes. A, Cardiomyocyte viability after treatment with metformin (1, 10, or 100 μmol/L) and exposure to H_2O_2 (50 μmol/L). B, Time (0, 5, 15, 30, 60, 120 minutes) -dependent changes in AMPK phosphorylation in cardiomyocytes after treatment with metformin (10 μmol/L). C, Dose-dependent changes in AMPK phosphorylation in cardiomyocytes after treatment with metformin (0.1, 1, 10, or 100 μmol/L). D, Effect of an AMPK inhibitor (compound C; 20 μmol/L) on cardiomyocyte viability after treatment with metformin (10 μmol/L). E, Effect of an AMPK activator (AICAR; 500 μmol/L) on cardiomyocyte viability after treatment with metformin (10 μmol/L). Values are mean±SEM. P-AMPKα indicates phosphorylation of AMPKα. *$P<0.05$ vs no treatment; †$P<0.05$ vs H_2O_2 (50 μmol/L) treatment.

effects[16] and may alleviate mechanical or neurohormonal stress on the heart.

Clinical Perspective on p 2577

These findings led us to hypothesize that activation of AMPK by metformin may exert a cardioprotective effect under stress conditions. Accordingly, metformin might be a potential new treatment for cardiac failure because it activates AMPK and increases NO production. Therefore, we investigated the influence of metformin on apoptosis, an important feature of heart failure, using cultured neonatal cardiomyocytes exposed to H_2O_2 and the effect of metformin on the progression of pacing-induced heart failure in dogs, along with activation of AMPK.

Methods

Experimental procedures are described in the online-only Data Supplement.

Statistical Analysis

Results are expressed as mean±SEM. Comparison of changes between groups over time was performed by 2-way repeated-measures ANOVA. Other data were compared between groups by 1-way fractional ANOVA. The Tukey-Kramer test was used to correct for multiple comparisons. In all analyses, values of $P<0.05$ were considered to indicate statistical significance.

The authors had full access to and take full responsibility for the integrity of the data. All authors have read and agree to the manuscript as written.

Results

Metformin Attenuates Oxidative Stress–Induced Cell Death and Apoptosis in Cultured Cardiomyocytes via AMPK Activation

Cell viability was decreased in the presence of H_2O_2, as shown by the MTT assay, but this change was blunted by treatment with metformin in a dose-dependent manner (Figure 1A). Treatment with metformin (10 μmol/L) stimulated phosphorylation of AMPK in cultured cardiomyocytes in a time- and dose-dependent manner (Figure 1B and 1C). The effect of metformin on cell viability was blunted by cotreatment with compound C, an AMPK inhibitor (20 μmol/L) (Figure 1D). 5-Amino-4-imidazole-1-β-D-carboxamide ribofuranoside (AICAR; another AMPK activator) had an effect similar to metformin on cardiomyocyte viability after exposure to H_2O_2 (Figure 1E). These results suggested that

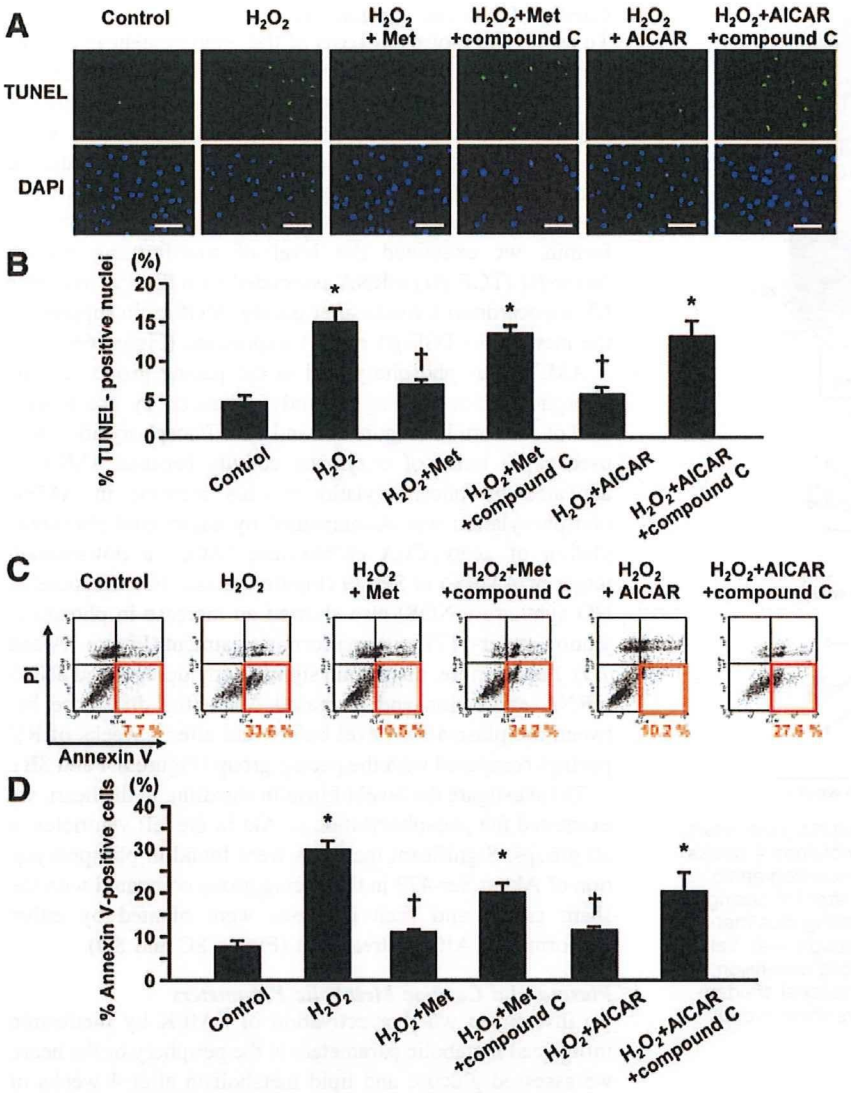

Figure 2. Effect of metformin on oxidative stress–induced apoptosis via AMPK activation in cultured rat cardiomyocytes. Representative (A) and quantitative (B) data on cardiomyocyte apoptosis obtained by TUNEL staining (n=3 in each experiment). Representative (C) and quantitative (D) data on cardiomyocyte apoptosis obtained by flow cytometry (n=3 in each experiment). Values are mean±SEM. PI indicates propidine iodide. *$P<0.05$ vs control; †$P<0.05$ vs H_2O_2 (50 μmol/L) treatment.

activation of AMPK protected cardiomyocytes against damage caused by H_2O_2.

H_2O_2 also increased cardiomyocyte apoptosis, as shown by the terminal deoxynucleotidyl transferase–mediated dUTP nick-end labeling (TUNEL) staining and flow cytometry (annexin V–positive and propidine iodide–negative cells) (Figure 2A through 2D). Metformin pretreatment significantly reduced the extent of cardiomyocyte apoptosis compared with that in untreated control cells (Figure 2A through 2D). Treatment with compound C inhibited the effects of metformin and AICAR (which was similar to that of metformin) on apoptosis in cardiomyocytes exposed to H_2O_2 (Figure 2A through 2D). These results suggested that the activation of AMPK by metformin could prevent apoptosis of cardiomyocytes induced by H_2O_2.

Effect of Metformin on Cardiac Function in Dogs With Pacing-Induced Heart Failure

Cardiac Physiological and Pathophysiological Parameters

Four weeks after the rapid right ventricular (RV) pacing, left ventricular (LV) end-diastolic dimension, LV end-systolic dimension, LV fractional shortening, and LV ejection fraction of the pacing group showed significant deterioration compared with the sham group (Figure 3A and 3B). Treatment with metformin significantly reduced both LV dimensions and increased both LV fractional shortening and LV ejection fraction compared with the pacing group (Figure 3A and 3B). Before RV pacing, both mean aortic pressure and heart rate were similar in all groups, and these parameters did not change throughout the study (Table). Four weeks after the RV pacing, pulmonary capillary wedge pressure, mean pulmonary artery pressure, and LV end-diastolic pressure were all significantly higher in the pacing group compared with the sham group (Figure 4A and 4B). Metformin treatment significantly reduced pulmonary capillary wedge pressure, mean pulmonary artery pressure, and LV end-diastolic pressure compared with the pacing group (Figure 4A and 4B). Furthermore, cardiac output was decreased and systemic vascular resistance was increased in the pacing group compared with the sham group, whereas metformin increased cardiac output and decreased systemic vascular resistance compared with the levels in the pacing group (the Table).

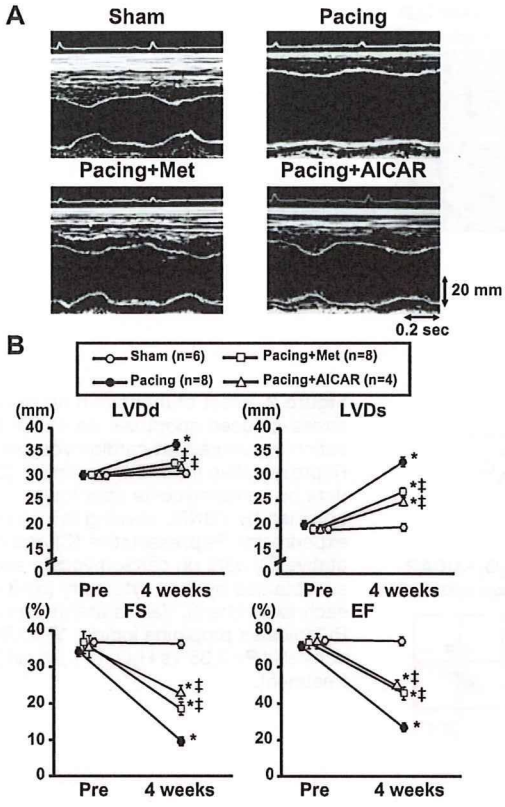

Figure 3. Effect of metformin on echocardiographic parameters. A, Representative M-mode echocardiograms obtained 4 weeks after sham surgery or after RV pacing. B, Echocardiographic parameters before and after sham surgery or after RV pacing in the sham group (n=6), pacing group (n=8), pacing plus metformin group (n=8), and pacing plus AICAR group (n=4). Values are mean±SEM. LVDd indicates LV end-diastolic dimension; LVDs, LV end-systolic dimension; LVFS, LV fractional shortening; and LVEF, LV ejection fraction. *$P<0.01$ vs sham group; ‡$P<0.01$ vs pacing group.

Importantly, the percentage of TUNEL-positive cells to total cells in LV myocardium in the pacing group increased compared with that in the sham group, which was blunted by treatment with either metformin or AICAR (Figure 5A through 5E).

Consistent with previous data,[17] no significant differences were found in body weight, the ratio of LV plus septal weight to body weight, and the ratio of RV weight to body weight among all groups (the Table).

To explore established markers of cardiac failure, we analyzed LV myocardial expression of the atrial natriuretic peptide and brain natriuretic peptide genes, which showed an increase in the pacing group, whereas metformin significantly suppressed this increase (Figure 6A and 6B). Metformin also significantly reduced the levels of angiotensin II and norepinephrine compared with the pacing group (the Table).

Pedometer counts were significantly reduced in the pacing group compared with the sham group, suggesting that heart failure led to reduced physical activities (the Table). Metformin increased the pedometer count compared with that in the pacing group. No differences in body fat were found among all groups (the Table).

Cardiac Molecular Parameters

To assess the molecular basis of the improvement in cardiac performance achieved by metformin administration for 4 weeks, we examined the collagen volume fraction in LV myocardium after staining with Masson's trichrome stain. Metformin reduced the collagen volume fraction compared with the pacing group (Figure 6C and 6D). To further investigate the mechanism of this antifibrotic effect of metformin, we examined the level of transforming growth factor-β1 (TGF-β1) mRNA associated with fibrosis in canine LV myocardium 4 weeks after pacing. Metformin suppressed the increase in TGF-β1 mRNA expression (Figure 6E).

AMPK was phosphorylated in the pacing group, and its phosphorylation was significantly enhanced by administration of metformin (Figure 7A and 7B). Phosphorylation was used as an index of enzymatic activity because AMPK is activated by phosphorylation.[18] This increase in AMPK phosphorylation was accompanied by augmented phosphorylation of acetyl-CoA carboxylase (ACC; a downstream target of AMPK) at Ser-79 (Figure 7A and 7C). Endothelial NO synthase (eNOS) also showed an increase in phosphorylation at Ser-1177 with metformin treatment (Figure 7A and 7D). Furthermore, metformin significantly upregulated eNOS mRNA expression and increased ΔNO (the difference between the plasma NO level before and after 4 weeks of RV pacing) compared with the pacing group (Figure 8A and 8B).

To investigate the level of insulin signaling in the heart, we examined the phosphorylation of Akt in the left ventricles in all groups. Significant increases were found in phosphorylation of Akt at Ser-473 in the pacing group compared with the sham group, and such increases were blunted by either metformin or AICAR treatment (Figure 8C and 8D).

Plasma and Cardiac Metabolic Parameters

To investigate whether activation of AMPK by metformin influenced metabolic parameters in the periphery or the heart, we assessed glucose and lipid metabolism after 4 weeks of pacing. Plasma free fatty acids tended to increase in the pacing group compared with the sham group, although no statistically significant difference was found. Fasting plasma levels of both glucose and lactate were similar among all groups (the Table). Both the fasting plasma insulin level and the homeostasis model assessment–insulin resistance value were significantly increased in the pacing group, whereas metformin reduced both parameters until they were similar to those of the sham group (the Table).

In the heart, both glucose extraction and the arterial–coronary sinus difference were increased in the pacing group compared with the sham group (the Table). In the pacing group, the free fatty acids extraction was not increased, but the arterial–coronary sinus difference tended to increase compared with the sham group (the Table). Lactate extraction and the arterial–coronary sinus difference were similar among all groups (the Table).

AICAR Mimics the Effect of Metformin in This Canine Pacing Model

To further confirm that activation of AMPK contributed to inhibition of the progression of heart failure, we administered

Table. Characteristics of the Dogs at 4 Weeks

	Sham Group (n=6)	Pacing Group (n=8)	Pacing+Metformin Group (n=8)	Pacing+AICAR Group (n=4)
Organ weight				
Body weight, kg	9.5±0.2	9.4±0.2	9.7±0.1	9.6±0.3
LV+septal weight, g	42±0.6	47.3±1.2	43.6±0.9	44.8±1.3
LV+septal weight/body weight ratio, g/kg	4.4±0.1	5.0±0.1	4.5±0.1	4.7±0.2
RV weight, g	14.7±0.5	15.6±0.6	15.0±1.2	14.7±1.0
RV weight/body weight ratio, g/kg	1.5±0.1	1.7±0.1	1.5±0.1	1.5±0.1
Hemodynamic parameters				
Mean aortic pressure, mm Hg	105±5	109±2	100±2	97±3.3
Heart rate, bpm	118±5	136±4	128±5	126±3.6
Cardiac output, L/min	2.6±0.1	1.6±0.1*	2.2±0.3†	2.2±0.3†
Systemic vascular resistance, dynes · s · cm^{-5}	3317±189	4769±235*	3775±334†	3763±237†
Plasma metabolic parameters				
Fasting glucose, mmol/L	5.3±0.3	5.3±0.1	5.3±0.1	5.3±0.2
Fasting insulin, μU/mL	14.2±3.3	67.6±13.7*	18.9±7.3†	24.4±10.5†
HOMA-IR	3.4±0.1	15.8±0.1*	4.4±0.1†	5.8±0.1†
Free fatty acids, μmol/L	305±67	716±68	554±101	595±69
Lactate, mmol/L	1.4±0.2	1.5±0.2	1.5±0.1	1.4±0.1
Cardiac metabolic substrates				
Glucose				
Arterial, mmol/L	5.8±0.1	6.4±0.2	6.6±0.1	6.6±0.4
Arterial–coronary sinus difference, mmol/L	0.6±0.1	1.6±0.3*	0.9±0.1	1.1±0.3
Extraction rate, %	10.5±1.2	28.6±4.7*	13.3±1.8	17.7±4.7
Free fatty acids				
Arterial, mmol/L	213.5±44.9	532.3±98.5*	312.8±56.6	294.5±22.8
Arterial–coronary sinus difference, mmol/L	90.4±13.2	153.7±20.6	99.0±9.1	103.2±20.6
Extraction rate, %	47.5±9.2	29.9±2.8	33.9±5.1	36.9±8.6
Lactate				
Arterial, mmol/L	1.8±0.1	1.9±0.3	2.3±0.7	1.8±0.8
Arterial–coronary sinus difference, mmol/L	1.2±0.3	1.0±0.2	1.3±0.5	1.1±0.4
Extraction rate, %	62.6±16.0	48.2±3.8	55.0±12.2	61.8±6.9
Plasma neurohormone levels				
Norepinephrine, pg/mL	34.9±13.0	195.9±21.3*	59.2±11.2†	79.3±8.9†
Angiotensin II, pg/mL	34.7±15.0	153.6±24.3*	78.1±14.8†	73.4±11.8†
Body fat and activity				
Body fat, %	13.7±1.2	18.7±2.9	16±1.2	14.3±0.8
Pedometer count	88 783±2899	64 541±2530*	78 423±3292†	77 716±1472†

HOMA-IR indicates homeostasis model assessment–insulin resistance. Values are mean±SEM.
*$P<0.05$ vs the sham group; †$P<0.05$ vs the pacing group.

another AMPK activator (AICAR at a dose of 5 mg/kg SC every other day) to dogs. As expected, AICAR reproduced the effects of metformin in this canine pacing model (Figures 3 through 8).

Discussion

To the best of our knowledge, this is the first study to demonstrate clearly that long-term (not short-term) oral administration of metformin, which is used as an antidiabetic agent worldwide, inhibits cardiac remodeling and prevents the progression of heart failure in dogs, along with increases in AMPK activation and NO production. Of course, we and others have previously shown that in rodent either AMPK activation or NO production attenuates myocardial ischemia/reperfusion injury in the ischemic model[7–9] and prevents cardiac remodeling in the pressure overload model.[11,12,19,20] However, it has been unclear whether AMPK or NO can modulate cardiac remodeling and inhibit the progression of heart failure in a canine model with another pathogenic mechanism that is not an ischemic or a pressure overload heart failure model. Therefore, we used a rapid pacing-induced heart failure dog model, which is considered to be similar to human dilated cardiomyopathy[21,22] and can be superimposed on translational study for human heart failure.

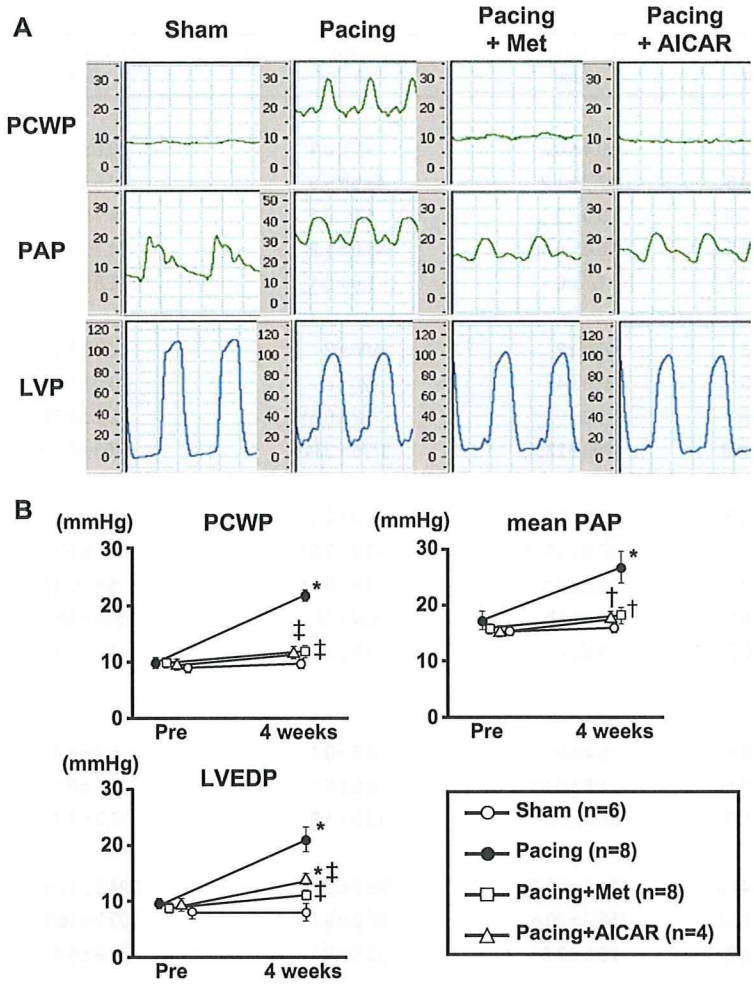

Figure 4. Effect of metformin on hemodynamic parameters. A, Representative graphs of hemodynamic parameters obtained at 4 weeks. B, Hemodynamic parameters before and after the 4-week study period in the sham (n=6), pacing (n=8), pacing plus metformin (n=8), and pacing plus AICAR (n=4) groups. Values are mean±SEM. PAP indicates pulmonary artery pressure; PCWP, pulmonary capillary wedge pressure; and LVEDP, LV end-diastolic pressure. *$P<0.05$ vs sham group; †$P<0.05$ vs pacing group; ‡$P<0.01$ vs pacing group.

Furthermore, we provide sufficient insight because dogs can be monitored more precisely for hemodynamic data than rodents.

Possible Cardioprotective Mechanism of Metformin Mediated via AMPK

Metformin has previously been shown to reduce high fat–induced apoptosis,[23] and AMPK has been reported to protect against hypoxic apoptosis in cardiomyocytes through attenuation of endoplasmic reticulum stress.[24] Consistent with these previous reports, we confirmed that metformin could ameliorate oxidative stress–induced apoptosis in cardiomyocytes. This effect was blunted by compound C, an AMPK inhibitor, suggesting that activation of AMPK was responsible for the inhibition of cardiomyocyte apoptosis. Furthermore, using a dog model, we demonstrated that metformin ameliorated the progression of heart failure induced by rapid RV pacing and decreased apoptosis in the LV myocardium, as indicated by TUNEL staining. Interestingly, AICAR, another AMPK activator, had effects almost identical to those of metformin, supporting that the activation of AMPK contributed to the observed cardioprotective effect. Indeed, AICAR also has been reported to reduce myocardial ischemia/reperfusion injury in humans and animals.[25,26] What processes following AMPK activation are involved in cardioprotection?

The first possibility is enhancement of NO production. Recchia et al[27] reported that basal cardiac NO release is decreased in dogs with heart failure induced by rapid pacing. We found that the difference in plasma NO levels between baseline and 4 weeks of RV pacing was significantly increased by metformin treatment compared with the pacing group. Metformin has been shown to phosphorylate AMPK at Thr-172 in cardiomyocytes and murine hearts,[4,5] whereas AMPK is known to phosphorylate eNOS at Ser-1177 in rat hearts,[28] resulting in an increase in NO production. Indeed, a recent report has indicated that short-term metformin treatment protects against myocardial infarction via AMPK-eNOS–mediated signaling in mice.[7] Other studies have suggested involvement of the AMPK-eNOS pathway in the response of endothelial cells to shear stress,[29] metformin,[30] and statins.[31] Consistent with these reports, we found that either metformin or AICAR promoted the phosphorylation of eNOS at Ser-1177 and increased both mRNA and protein levels of eNOS, possibly leading to increased plasma NO levels and reduced systemic vascular resistance. Although the precise mechanism of the effects of phosphorylation of AMPK by either metformin or AICAR on eNOS protein expression is not clear, these findings suggest that metformin or AICAR increased NO production, which improves endothelial

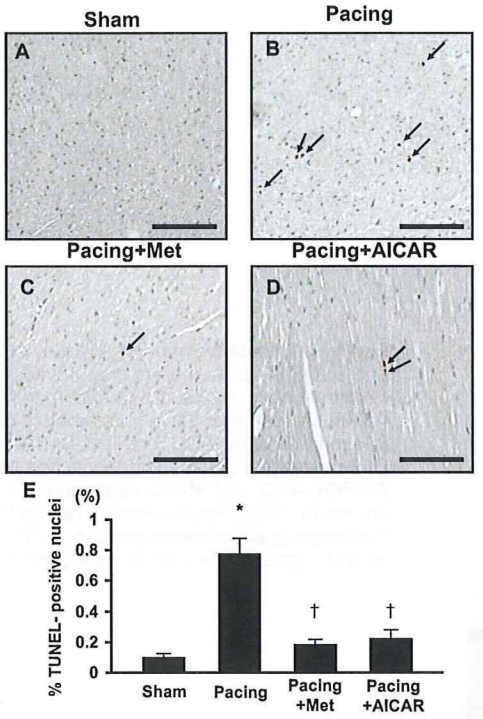

Figure 5. TUNEL staining of canine hearts at 4 weeks. Representative examples of TUNEL-stained hearts from sham (A), pacing (B), pacing plus metformin (C), and pacing plus AICAR (D) groups. Arrows indicate TUNEL-positive nuclei (brown). Scale bar=100 μm. E, Quantitative data on the percentage of TUNEL-positive nuclei to total cell nuclei. *$P<0.05$ vs sham group; †$P<0.05$ vs pacing group.

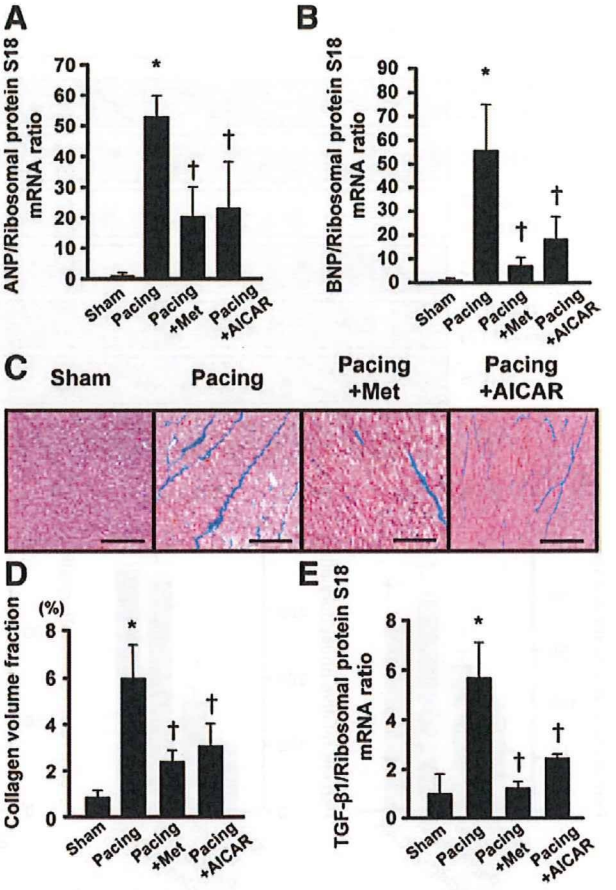

Figure 6. Natriuretic peptide expression, cardiac collagen volume fraction, and TGF-β1 expression. A, B, and E, Quantitative real-time reverse-transcriptase polymerase chain reaction analysis of myocardial atrial natriuretic peptide (ANP), brain natriuretic peptide (BNP), and TGF-β1 expression, respectively. The mRNA values were corrected for the ribosomal protein S18 mRNA level. The sham group was arbitrarily assigned a value of 1.0. Results are mean±SEM. Representative results from 3 independent experiments are shown. *$P<0.05$ vs sham group; #$P<0.05$ vs pacing group. C, Representative histological appearance of LV myocardium stained with Masson's trichrome stain (light blue). Scale bar=100 μm. D, Collagen volume fraction in the LV myocardium. Values are mean±SEM. *$P<0.05$ vs sham group; †$P<0.05$ vs pacing group.

function. NO is believed to have various cardioprotective effects.[16] Therefore, enhancement of NO production by metformin via activation of AMPK may have contributed to alleviating the progression of heart failure induced by rapid RV pacing.

The second possibility is related to the improvement in insulin resistance. It is known that insulin resistance is associated with the progression of chronic heart failure, whereas chronic heart failure may provoke insulin resistance by increasing sympathetic activity, activating the renin-angiotensin system, or both.[32,33] We found that rapid RV pacing for 4 weeks induced heart failure and that metformin treatment improved insulin resistance (estimated by homeostasis model assessment–insulin resistance) compared with the pacing group, suggesting that the beneficial effect of metformin on heart failure mediated via AMPK may have been due in part to an improvement in insulin resistance.

The third possibility is the metabolic effects of AMPK activation. Both metformin and AICAR are reported to increase glucose extraction in heart,[34,35] which may decrease the severity of the failing hearts. However, we found a 2- to 3-fold increase in myocardial glucose extraction of pacing dogs, and metformin returned glucose extraction to the value of the sham group. Numerous studies have shown a switch from free fatty acids to glucose as the primary energy substrate in humans and animals with advanced heart failure,[27,36–38] suggesting that the reduction in glucose extraction by the improvement in heart failure by AMPK activation is likely to be greater than the induction of glucose extraction by direct activation of AMPK. The possibility exists that AMPK-induced glucose extraction triggers the improvement in heart failure, followed by the restoration of metabolic switch. On the other hand, we found that the net free fatty acids extraction of the pacing group tended to increase despite no statistical significance, which is consistent with the report by Paolisso et al[39] that myocardial free fatty acids extraction increased in patients with congestive heart failure[39] but is contrary to the reports of the metabolic switch.[27,36–38] The metabolic switch may differ in relatively acute or chronic heart failure and by the severity of heart failure.

The increased phosphorylation of Akt in the pacing group was attenuated in either the pacing plus metformin or the pacing plus AICAR group, suggesting that the levels of activation of insulin signaling decreased in either the

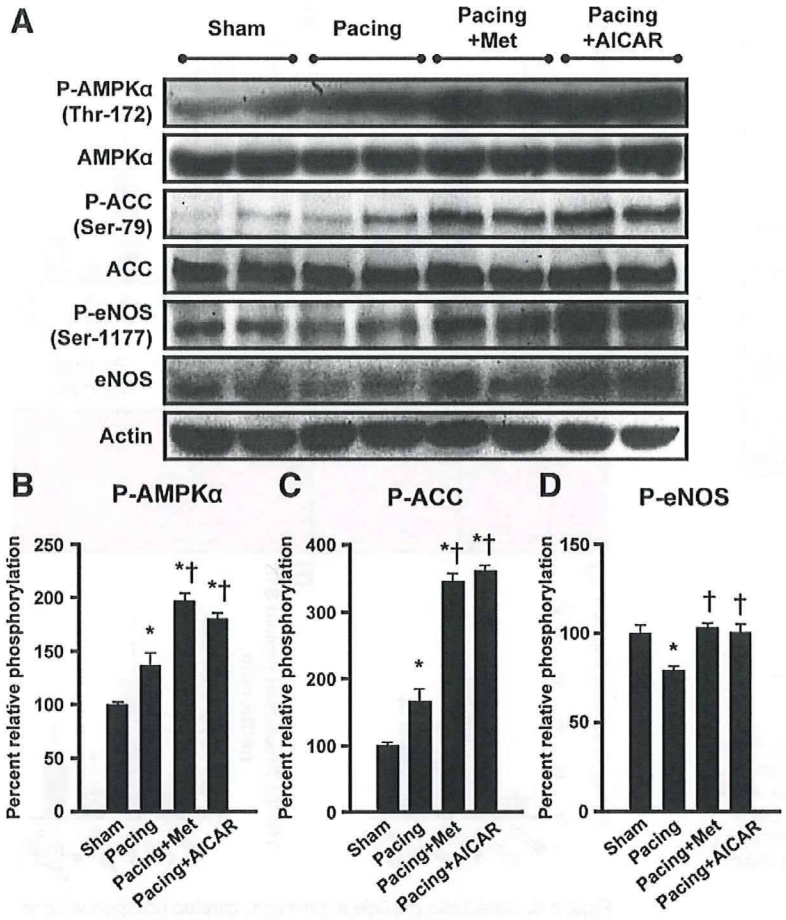

Figure 7. Phosphorylation of AMPKα, ACC, and eNOS in canine hearts after 4 weeks of treatment with or without metformin and AICAR. A, Representative immunoblots of phospho-AMPKα, ACC, and eNOS. B through D, Percentage relative phosphorylation of AMPKα, ACC, and eNOS, respectively. Values are mean±SEM. Representative results from 3 independent experiments are shown. *P<0.05 vs sham group; †P<0.05 vs pacing group.

metformin- or AICAR-treated group. Considering that glucose extraction was decreased in the pacing plus metformin and pacing plus AICAR groups and that AMPK was phosphorylated by either metformin or AICAR, which may increase in glucose extraction in the heart, the present data may be contradictory, but they are not contradictory when we consider the changes in phosphorylated Akt. The reason is that in this pacing-induced canine heart failure model, glucose extraction in the heart was influenced predominantly by insulin resistance, accompanied by the severity of heart failure, rather than AMPK phosphorylation, although further investigation on this issue is needed.

The fourth possibility is the antifibrotic effect of metformin. Several studies have indicated that AMPK activation inhibits protein synthesis through effects on both the eEF-2 and mTOR pathways.[40,41] We demonstrated that no significant difference in ventricular mass existed at autopsy among the groups. This dog pacing model has been reported to preserve wall thickness without hypertrophy or a consistent increase in heart weight, unlike the pressure overload model.[42] We found that metformin attenuated fibrosis and reduced the TGF-β1 mRNA level after 4 weeks of RV pacing compared with the pacing group. Metformin also improved representative markers of heart failure, including LV end-diastolic pressure, brain natriuretic peptide, angiotensin II, and norepinephrine. Although a number of factors may have contributed to the antifibrotic effect of metformin, our data suggest that inhibition of TGF-β1 by metformin has at least some role, resulting in the prevention of heart failure.

Taken together, these data suggest that metformin has a direct cardioprotective effect, has effects on the improvements of peripheral vascular system and insulin resistance, and inhibits fibrosis. All these actions might contribute to the improvement in the pathophysiology of heart failure, although we could not identify the exact role of each factor. It remains to be determined whether these results were a cause or consequence of improved cardiac function, especially in systemic effects of both insulin resistance and systemic vascular resistance.

Study Limitations

We found that the extent of phosphorylation of eNOS decreased despite the increase in the phosphorylated Akt in the pacing-induced failing canine hearts, which may be contradictory to previous reports that the phosphorylation of Akt leads to eNOS phosphorylation.[43,44] Because the signal transduction to modulate eNOS is unclear in the failing myocardium and the pathophysiological role and importance of Akt also are unclear, this discrepancy should be clarified in future studies.[45]

We need to consider the dose of metformin used in the present study, which was at least 3-fold higher than that used clinically. Nevertheless, adverse effects such as hypoglycemia and lactic acidosis were not detected during the experiment.

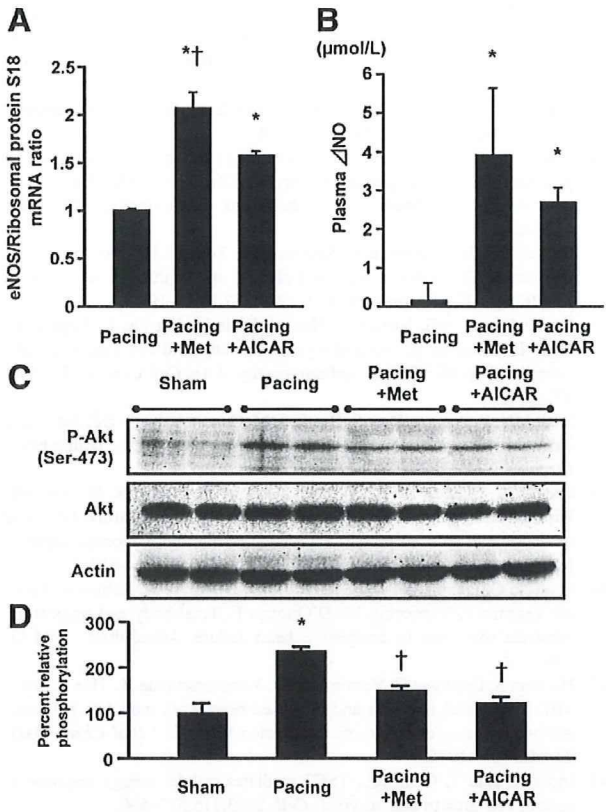

Figure 8. Effect of metformin on eNOS mRNA expression and plasma ΔNO levels, and phosphorylation of Akt in canine hearts. A, Quantitative real-time reverse-transcriptase polymerase chain reaction for eNOS mRNA. The mRNA levels were normalized to ribosomal protein S18 mRNA, and the pacing group was arbitrarily assigned a value of 1.0. B, Plasma ΔNO level after 4 weeks of RV pacing with or without metformin and AICAR administration. Values are mean±SEM. Representative results from 3 independent experiments are shown. *$P<0.05$ vs pacing group; †$P<0.05$ vs pacing plus AICAR group. C, Representative immunoblots of phospho-Akt. D, Percent relative phosphorylation of Akt. Values are mean±SEM. Representative results from 3 independent experiments are shown. *$P<0.05$ vs sham group; †$P<0.05$ vs pacing group.

Conclusions

We demonstrated that metformin prevents the progression of pacing-induced heart failure in dogs, along with the activation of AMPK. Metformin may offer a novel treatment strategy for heart failure.

Acknowledgments

We thank Yoko Horiguchi for her technical assistance; Dr Masafumi Myoishi for his assistance with TUNEL staining; Dr Hai Ying Fu for her assistance with flow cytometry; Dr Hatsue-Ishibashi-Ueda for her assistance with fluorescence microscopy; Dr Kyoko Shioya for her assistance with animal care; Tsunehisa Nakao (Nippon Shinyaku Co Ltd) for providing information about metformin; and the Evidence Finders' Club for their encouragement of this study.

Sources of Funding

This work was supported by grants in aid from the Ministry of Health, Labor, and Welfare–Japan and the Ministry of Education, Culture, Sports, Science and Technology–Japan and grants from the Japan Heart Foundation and the Japan Cardiovascular Research Foundation.

Disclosures

None.

References

1. Effect of intensive blood-glucose control with metformin on complications in overweight patients with type 2 diabetes (UKPDS 34): UK Prospective Diabetes Study (UKPDS) Group. *Lancet.* 1998;352:854–865.
2. Eurich DT, McAlister FA, Blackburn DF, Majumdar SR, Tsuyuki RT, Varney J, Johnson JA. Benefits and harms of antidiabetic agents in patients with diabetes and heart failure: systematic review. *BMJ.* 2007;335:497.
3. Zhou G, Myers R, Li Y, Chen Y, Shen X, Fenyk-Melody J, Wu M, Ventre J, Doebber T, Fujii N, Musi N, Hirshman MF, Goodyear LJ, Moller DE. Role of AMP-activated protein kinase in mechanism of metformin action. *J Clin Invest.* 2001;108:1167–1174.
4. Chan AY, Soltys CL, Young ME, Proud CG, Dyck JR. Activation of AMP-activated protein kinase inhibits protein synthesis associated with hypertrophy in the cardiac myocyte. *J Biol Chem.* 2004;279:32771–32779.
5. Zou MH, Kirkpatrick SS, Davis BJ, Nelson JS, Wiles WG 4th, Schlattner U, Neumann D, Brownlee M, Freeman MB, Goldman MH. Activation of the AMP-activated protein kinase by the anti-diabetic drug metformin in vivo: role of mitochondrial reactive nitrogen species. *J Biol Chem.* 2004;279:43940–43951.
6. Hardie DG. AMP-activated protein kinase: the guardian of cardiac energy status. *J Clin Invest.* 2004;114:465–468.
7. Calvert JW, Gundewar S, Jha S, Greer JJ, Bestermann WH, Tian R, Lefer DJ. Acute metformin therapy confers cardioprotection against myocardial infarction via AMPK-eNOS-mediated signaling. *Diabetes.* 2008;57:696–705.
8. Shibata R, Sato K, Pimentel DR, Takemura Y, Kihara S, Ohashi K, Funahashi T, Ouchi N, Walsh K. Adiponectin protects against myocardial ischemia-reperfusion injury through AMPK- and COX-2-dependent mechanisms. *Nat Med.* 2005;11:1096–1103.
9. Russell RR 3rd, Li J, Coven DL, Pypaert M, Zechner C, Palmeri M, Giordano FJ, Mu J, Birnbaum MJ, Young LH. AMP-activated protein kinase mediates ischemic glucose uptake and prevents postischemic cardiac dysfunction, apoptosis, and injury. *J Clin Invest.* 2004;114:495–503.
10. Tian R, Musi N, D'Agostino J, Hirshman MF, Goodyear LJ. Increased adenosine monophosphate-activated protein kinase activity in rat hearts with pressure-overload hypertrophy. *Circulation.* 2001;104:1664–1669.
11. Shibata R, Ouchi N, Ito M, Kihara S, Shiojima I, Pimentel DR, Kumada M, Sato K, Schiekofer S, Ohashi K, Funahashi T, Colucci WS, Walsh K. Adiponectin-mediated modulation of hypertrophic signals in the heart. *Nat Med.* 2004;10:1384–1389.
12. Liao Y, Takashima S, Maeda N, Ouchi N, Komamura K, Shimomura I, Hori M, Matsuzawa Y, Funahashi T, Kitakaze M. Exacerbation of heart failure in adiponectin-deficient mice due to impaired regulation of AMPK and glucose metabolism. *Cardiovasc Res.* 2005;67:705–713.
13. Bhalla RC, Toth KF, Tan E, Bhatty RA, Mathias E, Sharma RV. Vascular effects of metformin: possible mechanisms for its antihypertensive action in the spontaneously hypertensive rat. *Am J Hypertens.* 1996;9:570–576.
14. Marfella R, Acampora R, Verrazzo G, Ziccardi P, De Rosa N, Giunta R, Giugliano D. Metformin improves hemodynamic and rheological responses to L-arginine in NIDDM patients. *Diabetes Care.* 1996;19:934–939.
15. Katakam PV, Ujhelyi MR, Hoenig M, Miller AW. Metformin improves vascular function in insulin-resistant rats. *Hypertension.* 2000;35:108–112.
16. Rakhit RD, Marber MS. Nitric oxide: an emerging role in cardioprotection? *Heart.* 2001;86:368–372.
17. Komamura K, Shannon RP, Pasipoularides A, Ihara T, Lader AS, Patrick TA, Bishop SP, Vatner SF. Alterations in left ventricular diastolic function in conscious dogs with pacing-induced heart failure. *J Clin Invest.* 1992;89:1825–1838.
18. Lei B, Matsuo K, Labinskyy V, Sharma N, Chandler MP, Ahn A, Hintze TH, Stanley WC, Recchia FA. Exogenous nitric oxide reduces glucose transporters translocation and lactate production in ischemic myocardium in vivo. *Proc Natl Acad Sci U S A.* 2005;102:6966–6971.
19. Li HL, Yin R, Chen D, Liu D, Wang D, Yang Q, Dong YG. Long-term activation of adenosine monophosphate-activated protein kinase

attenuates pressure-overload-induced cardiac hypertrophy. *J Cell Biochem.* 2007;100:1086–1099.
20. Liao Y, Asakura M, Takashima S, Ogai A, Asano Y, Shintani Y, Minamino T, Asanuma H, Sanada S, Kim J, Kitamura S, Tomoike H, Hori M, Kitakaze M. Celiprolol, a vasodilatory beta-blocker, inhibits pressure overload-induced cardiac hypertrophy and prevents the transition to heart failure via nitric oxide-dependent mechanisms in mice. *Circulation.* 2004;110:692–699.
21. Elsner D, Riegger GA. Characteristics and clinical relevance of animal models of heart failure. *Curr Opin Cardiol.* 1995;10:253–259.
22. Lee WL, Chen JW, Ting CT, Ishiwata T, Lin SJ, Korc M, Wang PH. Insulin-like growth factor I improves cardiovascular function and suppresses apoptosis of cardiomyocytes in dilated cardiomyopathy. *Endocrinology.* 1999;140:4831–4840.
23. An D, Kewalramani G, Chan JK, Qi D, Ghosh S, Pulinilkunnil T, Abrahani A, Innis SM, Rodrigues B. Metformin influences cardiomyocyte cell death by pathways that are dependent and independent of caspase-3. *Diabetologia.* 2006;49:2174–2184.
24. Terai K, Hiramoto Y, Masaki M, Sugiyama S, Kuroda T, Hori M, Kawase I, Hirota H. AMP-activated protein kinase protects cardiomyocytes against hypoxic injury through attenuation of endoplasmic reticulum stress. *Mol Cell Biol.* 2005;25:9554–9575.
25. Mangano DT. Effects of acadesine on myocardial infarction, stroke, and death following surgery: a meta-analysis of the 5 international randomized trials: the Multicenter Study of Perioperative Ischemia (McSPI) Research Group. *JAMA.* 1997;277:325–332.
26. Kitakaze M, Takashima S, Minamino T, Node K, Shinozaki Y, Mori H, Kuzuya T, Hori M. Improvement by 5-amino-4-imidazole carboxamide riboside of the contractile dysfunction that follows brief periods of ischemia through increases in ecto-5-nucleotidase activity and adenosine release in canine hearts. *Jpn Circ J.* 1999;63:542–553.
27. Recchia FA, McConnell PI, Bernstein RD, Vogel TR, Xu X, Hintze TH. Reduced nitric oxide production and altered myocardial metabolism during the decompensation of pacing-induced heart failure in the conscious dog. *Circ Res.* 1998;83:969–979.
28. Chen ZP, Mitchelhill KI, Michell BJ, Stapleton D, Rodriguez-Crespo I, Witters LA, Power DA, Ortiz de Montellano PR, Kemp BE. AMP-activated protein kinase phosphorylation of endothelial NO synthase. *FEBS Lett.* 1999;443:285–289.
29. Zhang Y, Lee TS, Kolb EM, Sun K, Lu X, Sladek FM, Kassab GS, Garland T Jr, Shyy JY. AMP-activated protein kinase is involved in endothelial NO synthase activation in response to shear stress. *Arterioscler Thromb Vasc Biol.* 2006;26:1281–1287.
30. Davis BJ, Xie Z, Viollet B, Zou MH. Activation of the AMP-activated kinase by antidiabetes drug metformin stimulates nitric oxide synthesis in vivo by promoting the association of heat shock protein 90 and endothelial nitric oxide synthase. *Diabetes.* 2006;55:496–505.
31. Sun W, Lee TS, Zhu M, Gu C, Wang Y, Zhu Y, Shyy JY. Statins activate AMP-activated protein kinase in vitro and in vivo. *Circulation.* 2006; 114:2655–2662.
32. Swan JW, Anker SD, Walton C, Godsland IF, Clark AL, Leyva F, Stevenson JC, Coats AJ. Insulin resistance in chronic heart failure: relation to severity and etiology of heart failure. *J Am Coll Cardiol.* 1997;30:527–532.
33. Nielson C, Lange T. Blood glucose and heart failure in nondiabetic patients. *Diabetes Care.* 2005;28:607–611.
34. Fischer Y, Thomas J, Rosen P, Kammermeier H. Action of metformin on glucose transport and glucose transporter GLUT1 and GLUT4 in heart muscle cells from healthy and diabetic rats. *Endocrinology.* 1995;136: 412–420.
35. Russell RR 3rd, Bergeron R, Shulman GI, Young LH. Translocation of myocardial GLUT-4 and increased glucose uptake through activation of AMPK by AICAR. *Am J Physiol.* 1999;277:H643–H649.
36. Davila-Roman VG, Vedala G, Herrero P, de las Fuentes L, Rogers JG, Kelly DP, Gropler RJ. Altered myocardial fatty acid and glucose metabolism in idiopathic dilated cardiomyopathy. *J Am Coll Cardiol.* 2002;40: 271–277.
37. Sack MN, Rader TA, Park S, Bastin J, McCune SA, Kelly DP. Fatty acid oxidation enzyme gene expression is downregulated in the failing heart. *Circulation.* 1996;94:2837–2842.
38. Osorio JC, Stanley WC, Linke A, Castellari M, Diep QN, Panchal AR, Hintze TH, Lopaschuk GD, Recchia FA. Impaired myocardial fatty acid oxidation and reduced protein expression of retinoid X receptor-alpha in pacing-induced heart failure. *Circulation.* 2002;106:606–612.
39. Paolisso G, Gambardella A, Galzerano D, D'Amore A, Rubino P, Verza M, Teasuro P, Varricchio M, D'Onofrio F. Total-body and myocardial substrate oxidation in congestive heart failure. *Metabolism.* 1994;43: 174–179.
40. Horman S, Beauloye C, Vertommen D, Vanoverschelde JL, Hue L, Rider MH. Myocardial ischemia and increased heart work modulate the phosphorylation state of eukaryotic elongation factor-2. *J Biol Chem.* 2003; 278:41970–41976.
41. Inoki K, Zhu T, Guan KL. TSC2 mediates cellular energy response to control cell growth and survival. *Cell.* 2003;115:577–590.
42. Shinbane JS, Wood MA, Jensen DN, Ellenbogen KA, Fitzpatrick AP, Scheinman MM. Tachycardia-induced cardiomyopathy: a review of animal models and clinical studies. *J Am Coll Cardiol.* 1997;29: 709–715.
43. Montagnani M, Chen H, Barr VA, Quon MJ. Insulin-stimulated activation of eNOS is independent of Ca^{2+} but requires phosphorylation by Akt at Ser(1179). *J Biol Chem.* 2001;276:30392–30398.
44. Fulton D, Gratton JP, McCabe TJ, Fontana J, Fujio Y, Walsh K, Franke TF, Papapetropoulos A, Sessa WC. Regulation of endothelium-derived nitric oxide production by the protein kinase Akt. *Nature.* 1999;399: 597–601.
45. Shiojima I, Walsh K. Regulation of cardiac growth and coronary angiogenesis by the Akt/PKB signaling pathway. *Genes Dev.* 2006;20: 3347–3365.

CLINICAL PERSPECTIVE

Metformin is widely used as an antidiabetic drug with an insulin-sensitizing effect. A large-scale clinical trial (the UK Prospective Diabetes Study [UKPDS] 34) has shown that metformin therapy decreased the risk of cardiovascular death and the incidence of myocardial infarction associated with diabetes mellitus; metformin reduced the hemoglobin A_{1c} levels in treated patients to the same extent as in the other patients treated with conventional therapies. These results suggest that metformin might exert cardioprotective effects beyond its glucose-lowering action such as either activation of AMP-activated protein kinase (AMPK) or elevation of nitric oxide. Metformin is known to activate AMPK, which mediates potent cardioprotection against ischemia/reperfusion injury. AMPK also is activated in experimental failing myocardium, suggesting that activation of AMPK is beneficial for the pathophysiology of heart failure. The present study demonstrated that long-term oral administration of metformin prevents the progression of heart failure as indicated by hemodynamic and echocardiographic parameters. Metformin also promoted phosphorylation of both AMPK and endothelial nitric oxide synthase, increased plasma nitric oxide levels, and improved insulin resistance. As a result of these effects, metformin decreased apoptosis and improved cardiac function in failing canine hearts. Interestingly, another AMPK activator (AICAR) had effects equivalent to those of metformin, suggesting the primary role of AMPK activation in reducing apoptosis and preventing heart failure. Drugs that activate AMPK, especially metformin, may provide a novel strategy for the treatment of heart failure in clinical settings.

Autonomic Neuroscience: Basic and Clinical 148 (2009) 44–49

Contents lists available at ScienceDirect

Autonomic Neuroscience: Basic and Clinical

journal homepage: www.elsevier.com/locate/autneu

In vivo direct monitoring of vagal acetylcholine release to the sinoatrial node

Shuji Shimizu [a,c,d,*], Tsuyoshi Akiyama [b], Toru Kawada [a], Toshiaki Shishido [a], Toji Yamazaki [b], Atsunori Kamiya [a], Masaki Mizuno [a], Shunji Sano [c], Masaru Sugimachi [a]

[a] Department of Cardiovascular Dynamics, Advanced Medical Engineering Center, National Cardiovascular Center Research Institute, Osaka, Japan
[b] Department of Cardiac Physiology, National Cardiovascular Center Research Institute, Osaka, Japan
[c] Department of Cardiovascular Surgery, Okayama University Graduate School of Medicine, Dentistry and Pharmaceutical Sciences, Okayama, Japan
[d] Japan Association for the Advancement of Medical Equipment, Tokyo, Japan

ARTICLE INFO

Article history:
Received 30 September 2008
Received in revised form 16 February 2009
Accepted 23 February 2009

Keywords:
Heart rate
Vagal nerve activity
Acetylcholine
Sinoatrial node
Right atrium
Microdialysis
Anesthetized rabbit

ABSTRACT

To directly monitor vagal acetylcholine (ACh) release into the sinoatrial node, which regulates heart rate, we implanted a microdialysis probe in the right atrium near the sinoatrial node and in the right ventricle of anesthetized rabbits, and perfused with Ringer's solution containing eserine. (1) Electrical stimulation of right or left cervical vagal nerve decreased atrial rate and increased dialysate ACh concentration in the right atrium in a frequency-dependent manner. Compared to left vagal stimulation, right vagal nerve stimulation decreased atrial rate to a greater extent at all frequencies, and increased dialysate ACh concentration to a greater extent at 10 and 20 Hz. However, dialysate ACh concentration in the right atrium correlated well with atrial rate independent of whether electrical stimulation was applied to the right or left vagal nerve (atrial rate $= 304 - 131 \times \log[\mathrm{ACh}]$, $R^2 = 0.77$). (2) Right or left vagal nerve stimulation at 20 Hz decreased atrial rate and increased dialysate ACh concentrations in both the right atrium (right, 17.9 ± 4.0 nM; left, 7.9 ± 1.4 nM) and right ventricle (right, 0.9 ± 0.3 nM; left, 1.0 ± 0.4 nM). However, atrial dialysate ACh concentrations were significantly higher than ventricular concentrations, while ventricular dialysate ACh concentrations were not significantly different between right and left vagal nerve stimulation. (3) The response of ACh release to right and left vagal nerve stimulation was abolished by intravenous administration of a ganglionic blocker, hexamethonium bromide. In conclusion, ACh concentration in dialysate from the right atrium, sampled by microdialysis, is a good marker of ACh release from postganglionic vagal nerves to the sinoatrial node.

1. Introduction

Parasympathetic nerves play an important role in the regulation of heart rate under physiological conditions. To better understand the parasympathetic control of heart rate, it is important to quantitatively assess the efferent cardiac vagal nerve activity. Several methods have been used to assess this activity. Efferent cardiac vagal nerve electrical activity has been measured directly at the preganglionic site in several studies (Jewett, 1964; Kunze, 1972). We have developed a microdialysis technique which is used with high-performance liquid chromatography (HPLC) to monitor in vivo endogenous acetylcholine (ACh) release in the heart (Akiyama et al., 1994). Using this technique, we were able to monitor endogenous ACh release into the ventricular myocardium (Akiyama et al., 1994; Kawada et al., 2001). This technique permits the estimation of relative changes in postganglionic efferent cardiac vagal nerve activity in the ventricle.

However, vagal innervation is known to be heterogeneous in the heart. Kilbinger and Löffelholz (1976) reported that the ACh content of the ventricle was 41% and 19% of the atrial content in chicken and rabbit, respectively. Brown (1976) reported that ACh concentration was higher in the atrium than the ventricle, and that ACh content was higher in the right than the left portions in both the atrium and ventricle of the cat. Thus, to better understand the parasympathetic control of heart rate, which is the sinus rate under physiological conditions, we need information about the activities of postganglionic vagal nerves innervating the sinoatrial (SA) node.

In this study, we developed a dialysis probe using shorter dialysis fiber, which was suitable for implantation into the atrium. Using this dialysis probe, we tried to monitor myocardial interstitial ACh levels in the right atrium, especially near the SA node. Furthermore, we investigated whether the myocardial interstitial ACh levels reflect relative changes in activity of postganglionic vagal nerves innervating the SA node.

2. Materials and methods

2.1. Surgical preparation

Animal care was provided in accordance with the *Guiding Principles for the Care and Use of Animals in the Field of Physiological Sciences*

* Corresponding author. Department of Cardiovascular Dynamics, Advanced Medical Engineering Center, National Cardiovascular Center Research Institute, 5-7-1, Fujishiro-dai, Suita, Osaka, 565-8565 Japan. Tel.: +81 6 6833 5012; fax: +81 6 6835 5403.
E-mail address: shujismz@ri.ncvc.go.jp (S. Shimizu).

1566-0702/$ – see front matter © 2009 Elsevier B.V. All rights reserved.
doi:10.1016/j.autneu.2009.02.006

approved by the Physiological Society of Japan. All protocols were approved by the Animal Subject Committee of the National Cardiovascular Center. Forty-three Japanese white rabbits weighing from 2.2 to 2.9 kg were anesthetized using an intravenous injection of pentobarbital sodium (50 mg/kg) via the marginal ear vein, followed by a continuous intravenous infusion of α-chloralose and urethane (16 mg/kg/h and 100 mg/kg/h) through a catheter inserted into the femoral vein to maintain an appropriate level of anesthesia. The animals were intubated and ventilated mechanically with room air mixed with oxygen. Systemic arterial pressure was monitored by a catheter inserted into the femoral artery. Esophageal temperature, which was measured by a thermometer (CTM-303, TERUMO, Japan), was maintained between 38 and 39 °C using a heating pad. In all protocols, bilateral vagal nerves were exposed through a midline cervical incision and sectioned at the neck after the control dialysate sampling. A pair of bipolar stainless steel electrodes was attached to the efferent side of the right or left vagal nerve. The nerve and electrode were covered with warmed mineral oil for insulation. When vagal stimulation was required, the efferent vagal nerve was stimulated by a digital stimulator (SEN-7203, Nihon Kohden, Japan). The pulse duration and amplitude of nerve stimulation were set at 1 ms and 10 V.

With the animal in the lateral position, right lateral thoracotomy was performed and the right 3rd to 5th ribs were partially resected to expose the heart. After incision of the pericardium, stainless steel wires were attached to the apex and the anterior wall of the left ventricle for ventricular pacing. To prevent severe bradycardia and cardiac arrest induced by vagal stimulation, left ventricular pacing was performed at the same frequency as the heart rate before vagal stimulation. The ventricular rate was determined from the electrocardiogram using a cardiotachometer. Another pair of stainless steel wires was attached to the appendage of the right atrium for recording atrial electrocardiogram, from which atrial rate was determined. Heparin sodium (100 IU/kg) was administered intravenously to prevent blood coagulation. At the end of the experiment, animals were killed with an overdose injection of pentobarbital sodium. A postmortem examination confirmed that the dialysate probe did not penetrate into the atrial or ventricular cavity and the dialysis membrane was positioned totally within the atrial or ventricular wall.

2.2. Dialysis technique

The materials and properties of the dialysis probe have been described previously (Akiyama et al., 1994). Briefly, we designed a handmade transverse dialysis probe. A dialysis fiber of semipermeable membrane (4 mm length, 310 μm outer diameter, 200 μm inner diameter; PAN-1200, 50,000 molecular weight cutoff; Asahi Chemical, Tokyo, Japan) was attached at both ends to polyethylene tubes (25 cm length, 500 μm outer diameter, 200 μm inner diameter). A fine guiding needle (30 mm length, 510 μm outer diameter, 250 μm inner diameter) with a stainless steel rod (5 mm length, 250 μm outer diameter) was used for the implantation of the dialysis probe. In protocol 1 and 3, a dialysis probe was implanted in the right atrium near the junction between the superior vena cava and the right atrium. In protocol 2, a dialysis probe was also implanted in the right ventricular free wall. After implantation, the dialysis probe was perfused with Ringer's solution (NaCl 147 mM, KCl 4 mM, $CaCl_2$ 3 mM) containing the cholinesterase inhibitor eserine (100 μM) at a speed of 2 μl/min, using a microinjection pump (CMA/100, Carnegie Medicin, Sweden). Experimental protocols were started 120 min after implantation of the dialysis probe. We took account of the dead space between the dialysis membrane and the sample tube at the start of each dialysate sampling. Phosphate buffer (4 μl) containing an internal standard (isopropylhomocholine chloride) was transferred into each sample tube before dialysate sampling. Dialysate sampling periods were set at 10 min (1 sample volume = 20 μl).

2.3. Analytic procedure

Dialysate ACh was assayed using HPLC with electrochemical detection. An autosampler (CMA/200, Carnegie Medicin) was used. The HPLC system consisted of a pump with a pulse dumper (EP-300, Eicom, Japan), a separation column (AC-Gel, styrene polymer, 4 μm particle size, 2 mm inner diameter × 150 mm length, Eicom), an immobilized enzyme column (AC-Enzymepack, 1 mm inner diameter × 4 mm length, Eicom), an electrochemical detector (ECD-300, Eicom), and a degasser (DG-300, Eicom). The electrochemical detector was operated with a platinum working electrode at + 0.45 V vs. an Ag/AgCl reference electrode. The mobile phase was 50 mM potassium bicarbonate solution containing 400 mg/L of sodium 1-decansulfonate and 50 mg/L of disodium–EDTA. The pump flow rate was 0.15 ml/min.

Chromatograms were recorded and analyzed by an analog-to-digital converter (Power Chrom EPC-300, AD Instruments, Australia) with a computer. Concentrations of ACh and isopropylhomocholine chloride were determined by measuring the peak areas. The absolute detection limit of ACh was 10 fmol/injection (signal-to-noise ratio = 3).

2.4. Experimental protocols

2.4.1. Protocol 1

To examine whether atrial dialysate ACh concentration reflects ACh release from cardiac vagal nerves, we investigated the relationship between the dialysate ACh concentration in the right atrium and the frequency of right and left vagal nerve stimulation. We sampled control dialysate before and after vagal transection. Then we stimulated the right ($n = 8$) or left ($n = 8$) efferent vagal nerves for 10 min at frequencies of 5, 10, 20 and 40 Hz, and sampled dialysate during each stimulation. Ten minutes after vagal nerve stimulation, we sampled the dialysate again to check the recovery of ACh levels.

2.4.2. Protocol 2

To investigate the difference in vagal innervation density between the right atrium and right ventricle, we compared the atrial and ventricular dialysate ACh concentrations under control condition and during electrical vagal nerve stimulation. Control dialysates were sampled after vagal transection. Then the right ($n = 5$) or left ($n = 5$) efferent vagal nerve was stimulated for 10 min at a frequency of 20 Hz, and dialysates were collected during vagal stimulation.

2.4.3. Protocol 3

ACh is released from both pre- and post-ganglionic vagal nerves as a primary neurotransmitter. The cardiac vagal nerve ganglia are localized near the atrium (Löffelholz and Pappano, 1985). Electrical stimulation of cervical vagal nerves activates the entire efferent parasympathetic pathway, including both preganglionic and postganglionic nerves in the atrium. Thus it is possible that pre- and/or post-ganglionic nerves serve as the source of dialysate ACh. To determine whether pre- or post-ganglionic nerves are the source of atrial dialysate ACh, we observed ACh release in response to nerve stimulation before and after blockade of ganglionic transmission. We sampled control dialysate after vagal transection. Then we stimulated the right ($n = 9$) or left ($n = 8$) vagal nerve at a frequency of 20 Hz before and after intravenous administration of hexamethonium bromide (30 mg/kg) and sampled dialysate during vagal stimulation. To prevent severe hypotension induced by hexamethonium, arterial pressure was maintained by continuous intravenous infusion of phenylephrine (17.2 ± 1.6 μg/kg/min).

2.5. Statistical analysis

All data are presented as mean ± SE. For each protocol, heart rate and mean arterial pressure were compared by one-way repeated measures analysis of variance followed by a Dunnett's test against

control (Glantz, 2005). In protocol 1, we compared vagal stimulation-induced ACh release among the seven groups by one-way repeated measures analysis of variance followed by Tukey's test. Heart rates (atrial rate) and dialysate ACh concentrations during right and left vagal stimulation were compared by unpaired *t*-test. After logarithmic transformation of atrial dialysate ACh concentration, a linear regression analysis was performed to examine the relation between dialysate ACh concentration and atrial rate. In protocol 2, we compared atrial and ventricular dialysate ACh concentrations during vagal stimulation by two-way repeated measures analysis of variance. We also compared the effects of right and left vagal stimulation on atrial and ventricular dialysate ACh concentrations using an unpaired *t*-test. In protocol 3, we compared stimulation-induced ACh release with and without hexamethonium using one-way repeated measures analysis of variance followed by a Dunnett's test against control. Differences were considered significant at $P<0.05$.

3. Results

3.1. Protocol 1

Responses of heart rate and mean arterial pressure to electrical vagal nerve stimulation are shown in Table 1. Transection of bilateral vagal nerves did not change heart rate or mean arterial pressure significantly. While both right and left vagal stimulation decreased heart rate in proportion to the frequency of the stimulus, right vagal nerve stimulation decreased the heart rate to a greater extent than left vagal nerve stimulation at all stimulus frequencies tested ($P<0.05$ at 5 Hz, $P<0.01$ at 10 Hz, $P<0.05$ at 20 Hz and $P<0.05$ at 40 Hz). Heart rate recovered to the pre-stimulation levels after stimulation. Both right and left vagal nerve stimulation with ventricular pacing decreased mean arterial pressure. Mean arterial pressure recovered partially but remained lower than the pre-stimulation levels 10 min after stimulation.

Transection of bilateral vagal nerves did not change dialysate ACh concentration (Fig. 1). Both right and left vagal stimulation increased the dialysate ACh concentration in proportion to the stimulus frequency. Right vagal stimulation increased the dialysate ACh concentration from 1.9 ± 0.3 nM in the post-transection control to 2.7 ± 0.4 nM at 5 Hz ($P<0.05$ vs. control), 5.5 ± 0.8 nM at 10 Hz ($P<0.01$ vs. 5 Hz), 17.2 ± 3.0 nM at 20 Hz ($P<0.01$ vs. 10 Hz) and 40.4 ± 8.4 nM at 40 Hz ($P<0.01$ vs. 20 Hz). Dialysate ACh concentration recovered to 2.2 ± 0.3 nM 10 min after stimulation. Left vagal stimulation increased dialysate ACh concentration from 1.6 ± 0.3 nM in the post-transection control to 2.2 ± 0.4 nM at 5 Hz (N.S. vs. control), 3.2 ± 0.5 nM at 10 Hz ($P<0.01$ vs. control), 8.2 ± 1.4 nM at 20 Hz ($P<0.01$ vs. 10 Hz) and 24.7 ± 4.6 nM at 40 Hz ($P<0.01$ vs. 20 Hz). Dialysate ACh concentration recovered to 2.0 ± 0.5 nM 10 min after stimulation. While both right and left vagal stimulation increased dialysate ACh concentration in a frequency-dependent manner, right vagal nerve stimulation increased dialysate ACh concentration to a greater extent than left vagal nerve stimulation at 10 and 20 Hz (N.S. at 5 Hz, $P<0.05$ at 10 Hz, $P<0.05$ at 20 Hz and N.S. at 40 Hz).

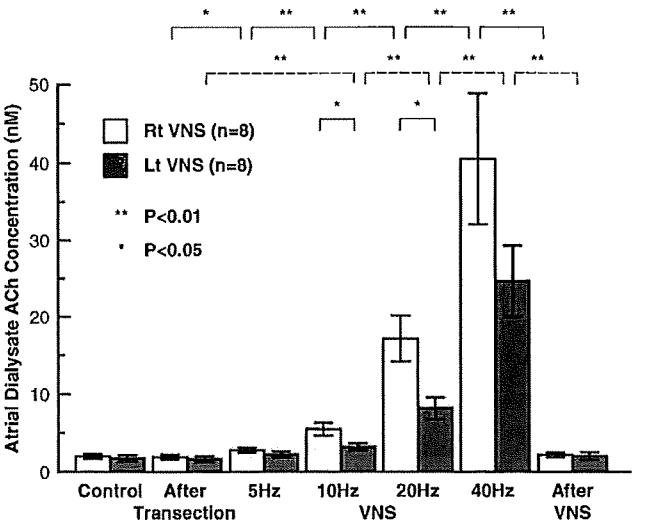

Fig. 1. Dialysate ACh concentrations of controls and during electrical vagal nerve stimulation at different frequencies. Right vagal nerve stimulation increased atrial dialysate ACh concentration from 1.9 ± 0.3 nM in the post-transection control to 2.7 ± 0.4 nM at 5 Hz, 5.5 ± 0.8 nM at 10 Hz, 17.2 ± 3.0 nM at 20 Hz and 40.4 ± 8.4 nM at 40 Hz. Left vagal nerve stimulation increased atrial dialysate ACh concentration from 1.6 ± 0.3 nM in the control to 2.2 ± 0.4 nM at 5 Hz, 3.2 ± 0.5 nM at 10 Hz, 8.2 ± 1.4 nM at 20 Hz and 24.7 ± 4.6 nM at 40 Hz. Values are means ± SE; Rt: right; Lt: left; VNS: electrical vagal nerve stimulation; *n*: number of rabbits: $^{**}P<0.01$, $^{*}P<0.05$.

The relationship between dialysate ACh concentration and atrial rate ($n=16$) is shown in Fig. 2. Dialysate ACh concentration in the right atrium correlated well with atrial rate (AR; $AR=304-131\times\log[ACh]$, $R^2=0.77$). There was no significant difference in the intercept or slope of regression line between right and left vagal nerve stimulation (right: $AR=304-135\times\log[ACh]$, $R^2=0.79$; left: $AR=303-126\times\log[ACh]$, $R^2=0.73$) (Glantz, 2005). The correlation between dialysate ACh concentration and atrial rate was independent of the side of vagal nerve stimulation.

Table 1
Responses of heart rate and mean arterial pressure to electrical vagal nerve stimulation (protocol 1).

	Heart rate (bpm)	Mean arterial pressure (mm Hg)
Rt vagal stimulation ($n=8$)	Atrial rate (pacing rate)	
Control before transection	298±8	83±4
Control after transection	293±7	85±6
VNS (5 Hz)	246±5** (296±5)	71±7
VNS (10 Hz)	201±6** (296±5)	77±6
VNS (20 Hz)	121±7** (296±5)	72±8
VNS (40 Hz)	88±4** (296±5)	65±7**
After VNS	287±10	70±9
Lt vagal stimulation ($n=8$)	Atrial rate (pacing rate)	
Control before transection	305±8	89±4
Control after transection	308±5	92±6
VNS (5 Hz)	267±6* (309±4)	79±6**
VNS (10 Hz)	236±10** (309±4)	82±6
VNS (20 Hz)	165±13** (309±4)	77±5**
VNS (40 Hz)	129±16** (309±4)	67±6**
After VNS	305±13	75±8**

Values are means ± SE; *n*: numbers of rabbits; Rt: right; Lt: left; VNS: electrical vagal nerve stimulation; $^{**}P<0.01$ vs. control; $^{*}P<0.05$ vs. control.

3.2. Protocol 2

Responses of heart rate and mean arterial pressure were similar to the responses to vagal stimulation at 20 Hz in protocol 1 (Table 2). Responses of ACh release in the right atrium and right ventricle to vagal stimulation are shown in Fig. 3. Right vagal stimulation increased the atrial dialysate ACh concentration from 2.6 ± 0.6 nM in the post-transection control to 17.9 ± 4.0 nM ($P<0.01$) and the ventricular dialysate ACh concentration from 0.4 ± 0.2 nM to 0.9 ± 0.3 nM ($P<0.01$). Left vagal stimulation also increased the atrial dialysate ACh concentration from 1.5 ± 0.4 nM to 7.9 ± 1.4 nM ($P<0.01$) and the ventricular dialysate ACh concentration from 0.3 ± 0.1 nM in the control to 1.0 ± 0.4 nM ($P<0.01$). Atrial dialysate ACh concentrations were higher than ventricular dialysate ACh concentrations in both right and left vagal stimulation ($P<0.01$). The interaction between the stimulation and the position of probe (atrium or ventricle) was significant ($P<0.01$). There was no difference in ventricular dialysate ACh concentration between right and left vagal stimulation, but atrial dialysate ACh concentration was significantly

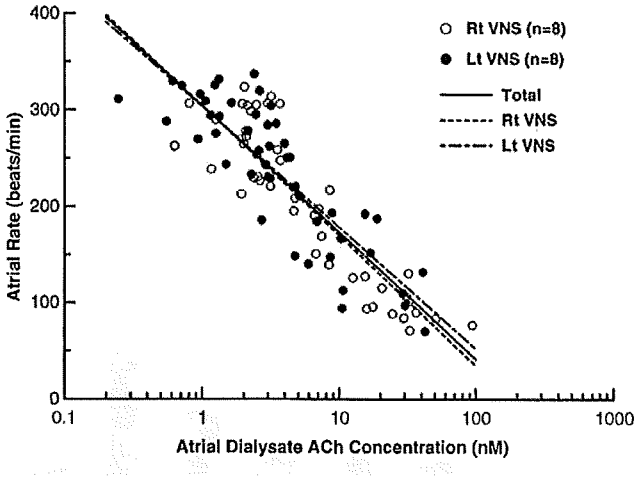

Fig. 2. Relation between dialysate ACh concentration (logarithmic scale) and atrial rate. Dialysate ACh concentration in the right atrium correlates well with atrial rate ($R^2=0.77$). Solid line, regression line fitting all 96 data points; dotted line, regression line fitting 48 data points of right vagal nerve stimulation; dot-dashed line, regression line fitting 48 data points of left vagal nerve stimulation. Rt: right; Lt: left; VNS: electrical vagal nerve stimulation.

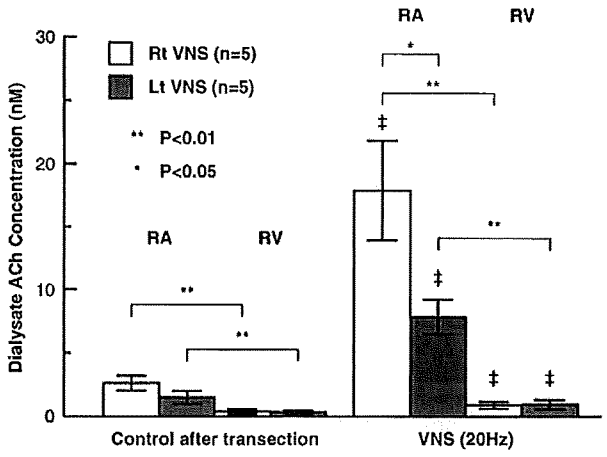

Fig. 3. Dialysate ACh concentrations in right atrium and right ventricle of controls and during electrical vagal nerve stimulation. Right vagal nerve stimulation significantly increased dialysate ACh concentration from 2.6±0.6 to 17.9±4.0 nM in the right atrium ($P<0.01$) and from 0.4±0.2 to 0.9±0.3 nM in the right ventricle ($P<0.01$). Left vagal nerve stimulation also increased dialysate ACh concentrations from 1.5±0.4 to 7.9±1.4 nM in the right atrium ($P<0.01$) and from 0.3±0.1 to 1.0±0.4 nM in the right ventricle ($P<0.01$). Dialysate ACh concentrations in the right atrium were significantly higher than those in the ventricle ($P<0.01$). Right vagal nerve stimulation increased atrial dialysate ACh concentration more than left vagal nerve stimulation ($P<0.05$). Values are means±SE; Rt: right; Lt: left; RA: right atrium; RV: right ventricle; VNS: electrical vagal nerve stimulation; n: number of rabbits; ‡$P<0.01$ vs. control; **$P<0.01$, *$P<0.05$.

higher during right vagal stimulation compared to left vagal stimulation ($P<0.05$).

3.3. Protocol 3

Responses of heart rate and mean arterial pressure are shown in Table 3. Both right and left vagal nerve stimulation decreased heart rate markedly before administration of hexamethonium. Administration of hexamethonium decreased heart rate significantly but mildly compared to control. Mean arterial pressure was maintained at pre-stimulation levels by continuous intravenous infusion of phenylephrine. After administration of hexamethonium, both right and left vagal nerve stimulation did not change the heart rate. Right vagal stimulation increased dialysate ACh concentration from 2.5±0.4 to 16.3±2.8 nM ($P<0.01$), but right vagal stimulation after administration of hexamethonium failed to increase ACh concentration (2.2±0.4 nM) compared to control. Likewise, left vagal stimulation increased dialysate ACh concentration from 1.5±0.3 to 8.7±1.4 nM ($P<0.01$), but left vagal stimulation after administration of hexamethonium did not increase ACh concentration (1.5±0.3 nM) compared to control (Fig. 4).

4. Discussion

We demonstrated that the microdialysis technique permitted in vivo monitoring of ACh release into the sinoatrial node from postganglionic cardiac vagal nerves. Dialysate ACh concentration in the right atrium correlated well with atrial rate and this correlation was independent of the side of vagal stimulation. These results indicate that in vivo monitoring of the myocardial interstitial ACh levels in the right atrium by microdialysis provides a useful strategy to obtain insights into the physiological roles of the vagal system in regulating heart rate.

Table 2
Responses of heart rate and mean arterial pressure to electrical vagal nerve stimulation (protocol 2).

	Heart rate (bpm)	Mean arterial pressure (mm Hg)
Rt vagal stimulation ($n=5$)	Atrial rate (pacing rate)	
Control after transaction	305±3	74±8
VNS (20 Hz)	122±4** (304±4)	65±9*
Control after VNS	300±3	68±8
Lt vagal stimulation ($n=5$)	Atrial rate (pacing rate)	
Control after transaction	306±5	95±3
VNS (20 Hz)	168±19** (308±5)	83±1**
Control after VNS	316±8	82±2**

Values are means±SE; n, numbers of rabbits; Rt: right; Lt: left; VNS: electrical vagal nerve stimulation; **$P<0.01$ vs. control; *$P<0.05$ vs. control.

4.1. Characteristics of atrial dialysate ACh concentration

With both right and left vagal nerve stimulation, the dialysate ACh concentration in the right atrium increased with increasing stimulus frequency and decreased to prestimulation levels after stimulation (Fig. 1). These results indicate that atrial dialysate ACh reflects ACh release from cardiac vagal nerves innervating the right atrium. Right vagal nerve stimulation decreased the atrial rate more than left stimulation at all stimulus frequencies, and right vagal nerve stimulation increased dialysate ACh concentration more than left stimulation at 10- and 20-Hz. The right atrium, including the SA node, is innervated not only by the right but also by the left vagal nerve. Ardell and Randall (1986) reported that supramaximal right and left

Table 3
Responses of heart rate and mean arterial pressure to electrical vagal nerve stimulation (protocol 3).

	Heart rate (bpm)	Mean arterial pressure (mm Hg)
Rt vagal stimulation ($n=9$)	Atrial rate (pacing rate)	
Control after transaction	292±9	70±8
VNS (20 Hz)	116±7** (299±5)	69±7
Hexamethonium iv	257±4**	84±7*
VNS after hexamethonium iv	257±4**	83±8*
Lt vagal stimulation ($n=8$)	Atrial rate (pacing rate)	
Control after transaction	317±3	79±3
VNS (20 Hz)	173±13** (313±4)	81±3
Hexamethonium iv	273±4**	87±5
VNS after hexamethonium iv	273±4**	87±4

Values are means±SE; n, numbers of rabbits; Rt: right; Lt: left; VNS: electrical vagal nerve stimulation; iv: intravenous administration; **$P<0.01$ vs. control; *$P<0.05$ vs. control.